Dear Editor,

Thank you very much for handling our manuscript (MS No.: acp-2020-576) submitted to Atmospheric Chemistry and Physics.

We have revised our manuscript very carefully based on the comments and suggestions from the reviewers. We have responded point-by-point to the comments by the reviewers and highlighted changes in the "tracking-changes" version of our manuscript.

We feel comments/suggestions by the reviewers have not only greatly improved the quality of our manuscript, but also enlightened us on our future works. While submitting the revised manuscript, we want to express our sincere appreciation and thanks to you and the referees for your hard works.

Thank you for your kind consideration.

Yours sincerely

Dr. Xinming Wang
State Key Laboratory of Organic Geochemistry
Guangzhou Institute of Geochemistry, Chinese Academy of Sciences
Guangzhou 510640, China.
E-mail: wangxm@gig.ac.cn

Dr. Xiang Ding
State Key Laboratory of Organic Geochemistry
Guangzhou Institute of Geochemistry, Chinese Academy of Sciences
Guangzhou 510640, China.
E-mail: xiangd@gig.ac.cn

Referee comment to acp-2020-576-RC1

The manuscript by Yu et al. reports one-year concurrent measurement of airborne PAHs at 12 sites across China. Size-segregated PAHs together with typical organic markers are measured to evaluate health risks of PAHs in different size particles and attribute emission sources of PAHs over different regions in China. The finding that toxic PAHs are concentrated in ultrafine particles is particularly interesting. The authors also find that PAH pollution is high in the northern China and nation-widely increases in wintertime, due to the unfavorable meteorological conditions and enhanced emissions of coal combustion and biomass burning. I think this is an important work nowadays in China as well in the global air pollution community. Overall this manuscript is well-organized and well-written and should be accepted after the authors address the minor issues below.

Major comments:

1. The PM samples were collected in 6 regions of China, including urban, sub-urban and remote sites. The authors are suggested to add more comparison of PAH concentrations and compositions among different types of sampling sites.

Reply: Thank you for your suggestion. In the revised manuscript, we add more discussion on $\sum_{24}$PAHs concentrations, compositions, sources and BaP_{eq} concentration and sources among different types of sampling sites. And Figure 1-4 were added in supporting information file and the revised manuscript as Figure S2, Figure S4, Figure S5 and Figure S6. Figure 5 and Figure 6 was added in the revised manuscript as Figure 7b and Figure 7e. (The line numbers here refers to the 'tracking changes' file)

"The concentrations of $\sum_{24}$PAHs at urban sites (82.7 ng m^{-3}) were significant higher ($p<0.05$)

than those at sub-urban (48.0 ng m^{-3}) and remote sites (18.0 ng m^{-3}) (Figure 1) (Line 228-229). And BeP_{eq} (Figure 2) and ILCR (Figure 3) were both the highest at urban sites. All these indicated that people in urban regions of China were faced with higher exposure risk of PAHs pollution as compared to those in rural and remote areas. Figure 4 exhibits that 4- and 5-rings PAHs are the majority in $\sum_{24}$PAHs at urban, sub-urban and remote sites, which totally accounted 72.2, 63.8 and 66.6% of the total amounts in TSP, respectively. The percentage of 5-rings PAHs dominates at urban sites, and 4-rings PAHs makes the largest proportion at sub-urban and remote sites (Line 244-250). PMF result showed that at urban and sub-urban sites coal combustion was the largest source of $\sum_{24}$PAHs (70.4 ng m^{-3}, 85.1% and 30.5 ng m^{-3}, 63.5%), followed by biomass burning (10.1 ng m^{-3}, 12.2% and 16.3 ng m^{-3}, 33.9%) and vehicle emission (2.2 ng m^{-3}, 2.6% and 1.2 ng m^{-3}, 2.5%), while at remote sites the contributions of coal combustion (9.1 ng m^{-3}, 50.6%) and biomass burning (7.8 ng m^{-3}, 43.7%) were comparable and vehicle emission (1.0 ng m^{-3}, 5.7%) had minor contributions (Figure 5) (Line 410-415). Coal combustion was the predominated source of BaP_{eq}, and its contribution at urban sites (8.3 ng m^{-3} and 96.4%) were larger than those at sub-urban (3.3 ng m^{-3} and 90.8%) and remote (1.0 ng m^{-3} and 82.5%) sites. (Figure 6)" (Line 426-428)

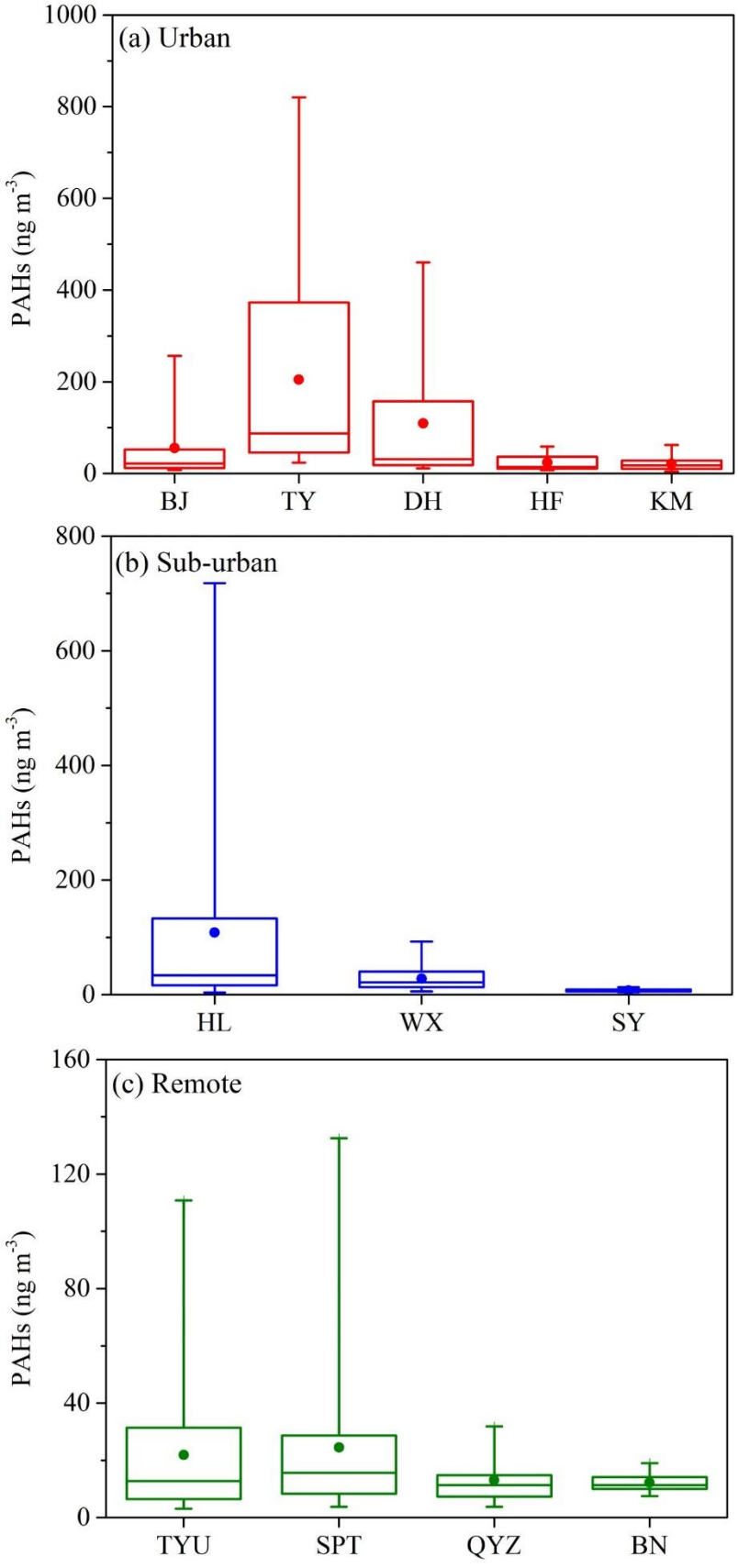

Figure 1 Concentrations of $\sum_{24}$PAHs at urban, sub-urban and remote sites.

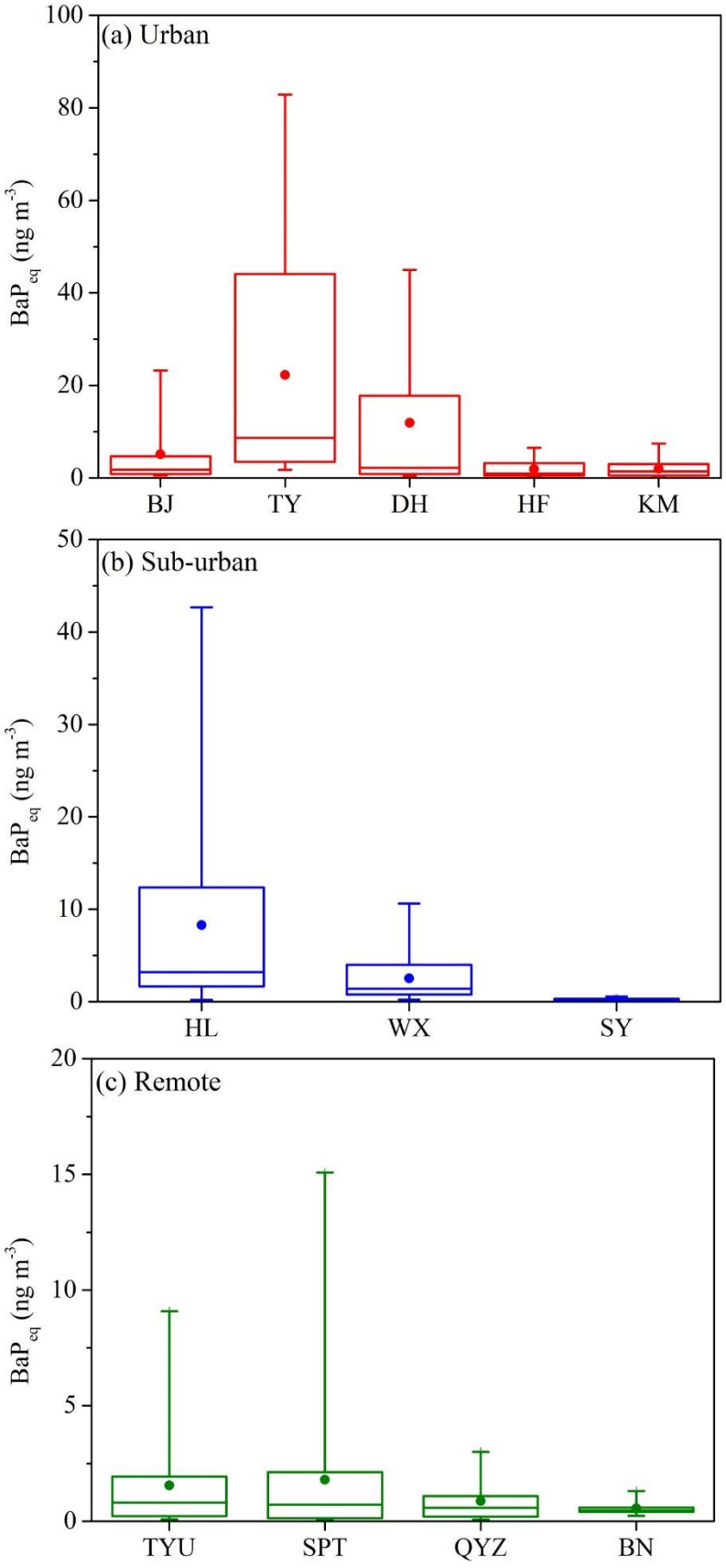

Figure 2 Concentrations of BaP_{eq} at urban, sub-urban and remote sites.

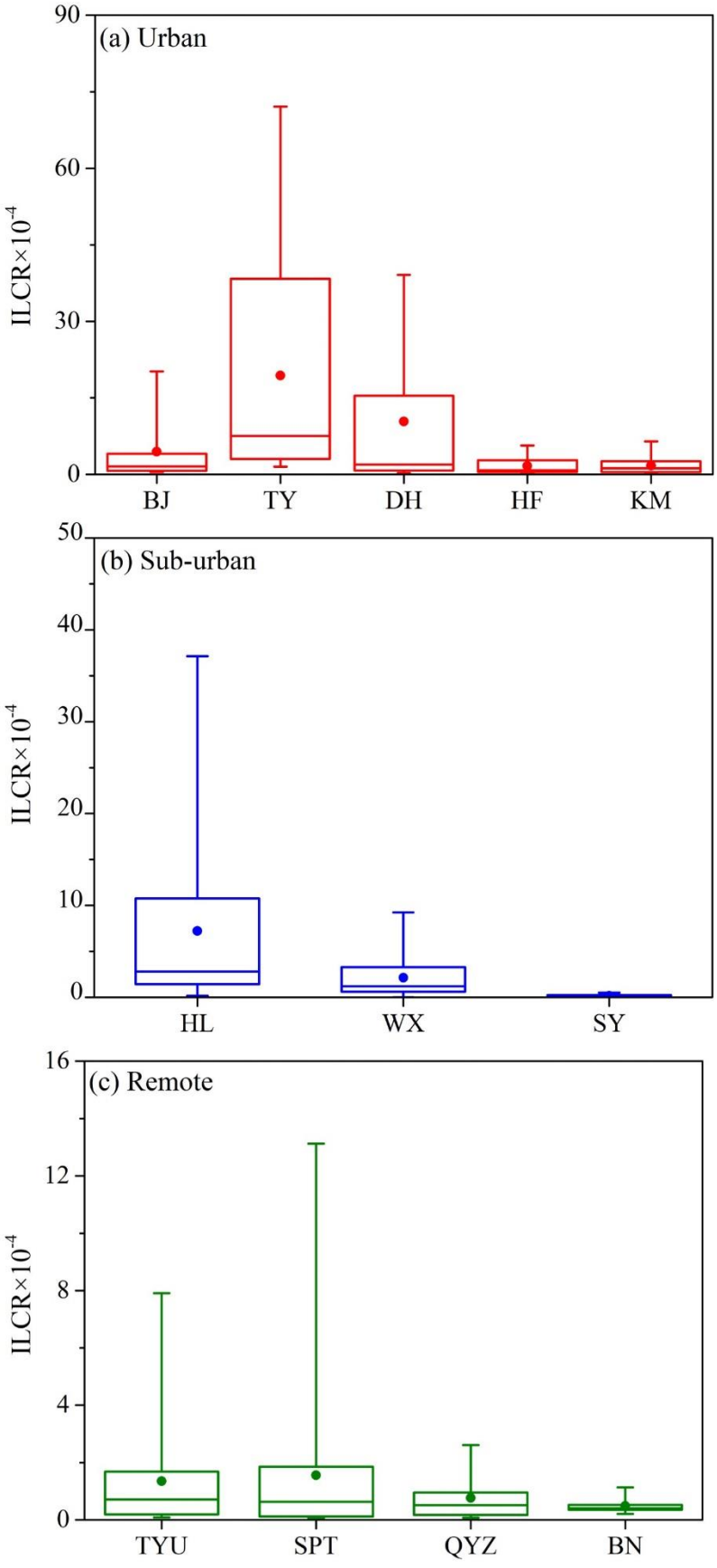

Figure 3 ILCR at urban, sub-urban and remote sites.

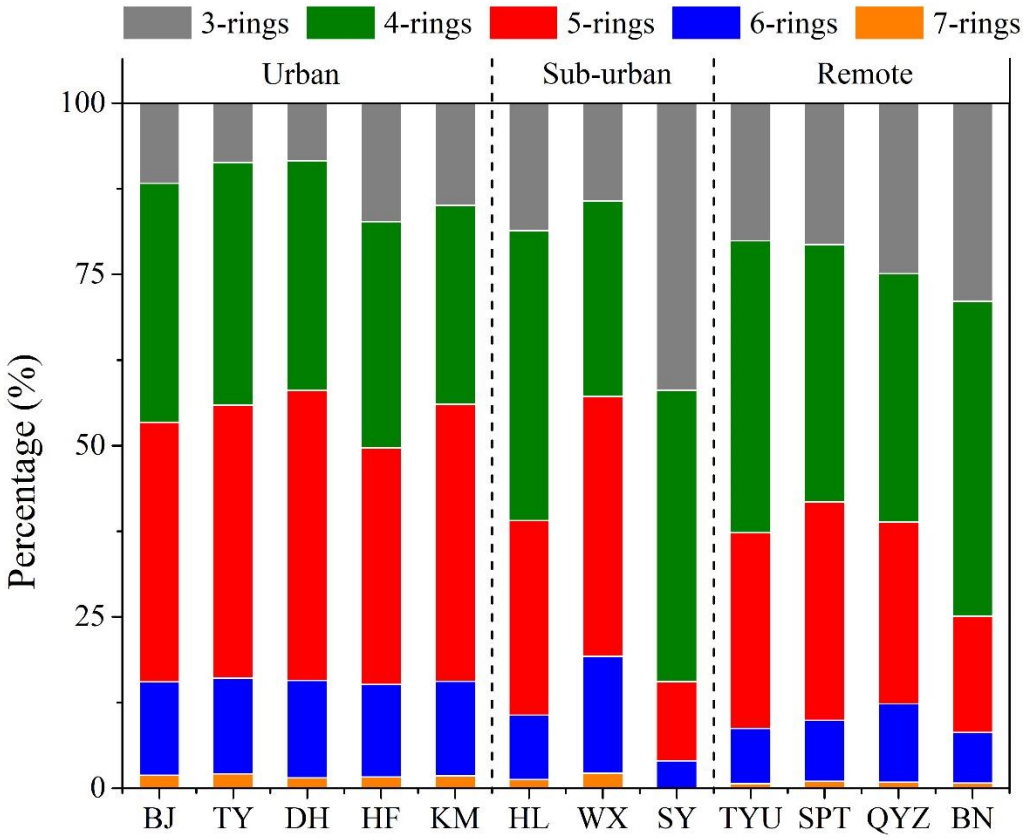

Figure 4 PAHs composition at urban, sub-urban and remote sites.

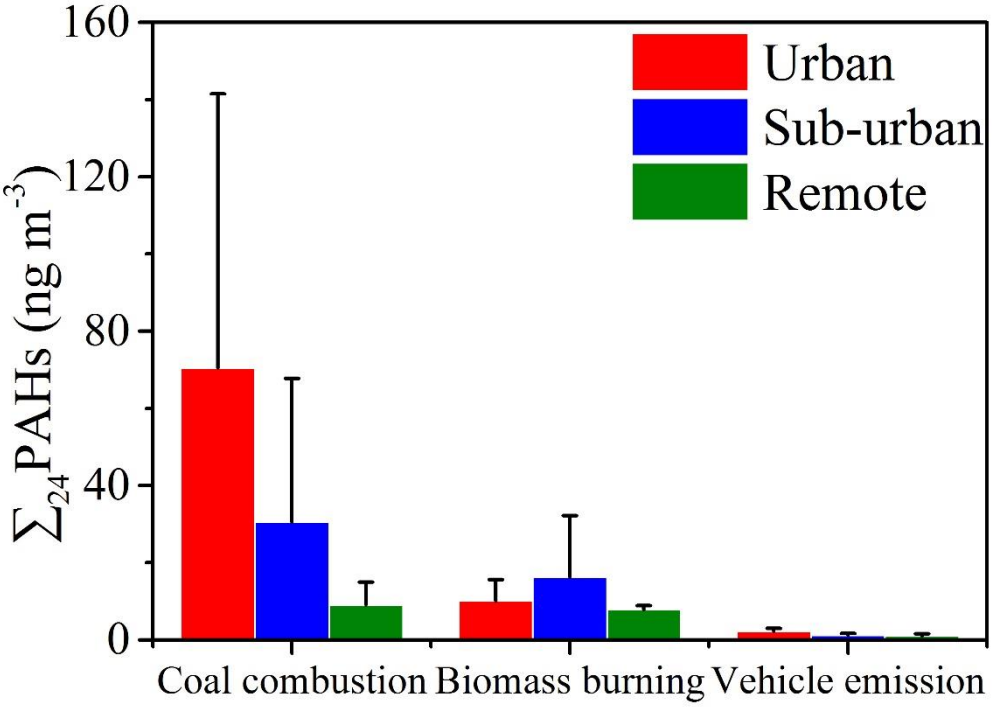

Figure 5 Difference of $\sum_{24}$PAHs sources at urban, sub-urban and remote sites.

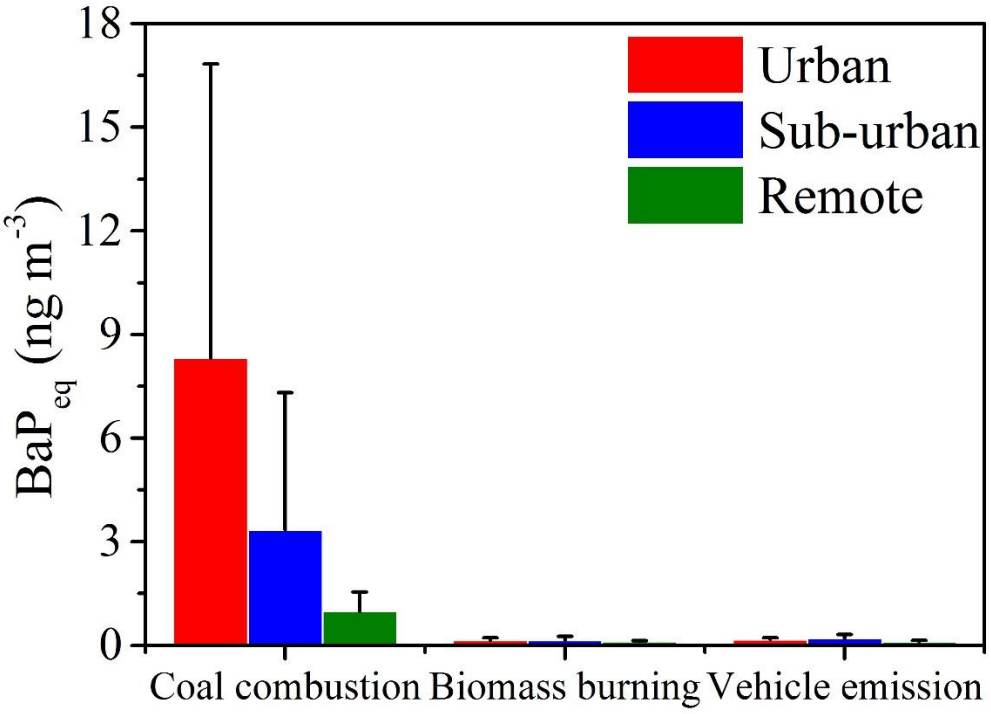

Figure 6 Difference of BaP_{eq} sources at urban, sub-urban and remote sites.

2. As I know, the national standard is not for BaP_{eq} but BaP. The authors should directly compare measured BaP levels with the national standard.

Reply: Yes, the national standard (1.0 ng m^{-3}) is for BaP. In the revised manuscript, we directly compare measured BaP levels with the national standard.

"Annual averages of BaP in TSP among the 12 sites were in the range of 0.09 to 11.0 ng m^{-3} with a mean of 2.58 ng m^{-3}. The highest level of atmospheric BaP occurred at TY and the lowest existed at SY. The BaP values at five sites (WX, BJ, HL, DH and TY) exceeded the national standard of annual atmospheric BaP (1.0 ng m^{-1}) by factors of 1.2 to 11.0. For BaP_{eq}, annual averages ranged from 0.21 to 22.2 ng m^{-3} with the predominant contribution from 5-rings PAHs (Figure 1b)." (Line 230-235)

Specific comments:

1. Line 52. Replace “associated” to “was associated”.

Reply: Revised as suggested. (Line 57)

2. Line 57. Replace “enriches” to “enrich”.

Reply: Revised as suggested. (Line 62)

3. Line 58. Replace “and” to “which”.

Reply: Revised as suggested. (Line 63)

4. Line 91. Delete “in”.

Reply: Revised as suggested. (Line 96)

5. Line 133. Replace “8h” to “8 h”.

Reply: Revised as suggested. (Line 144)

6. Line 146. Replace “3.3μm” to “3.3 μm”.

Reply: Revised as suggested. (Line 161)

7. Line 190. Replace “site” to “sites”.

Reply: Revised as suggested. (Line 207)

8. Line 214.The unit is misspelling. It should be “ng m^{-3}”.

Reply: Revised as suggested.

9. Line 259. Replace “high” to “higher”.

Reply: Revised as suggested. (Line 294)

10. Line 264. The abbreviation of boundary layer height is “BLH”. Please replace “BHL” to “BLH” throughout the manuscript.

Reply: Revised as suggested. (Line 307, Line 309, Line 311, Line 316, Line 446, Line 788)

11. Line 281. Replace “within each northern region” to “within each region in the northern China”.

Reply: Revised as suggested. (Line 330-331)

12. Line 299. Replace “high” to “higher”.

Reply: Revised as suggested. (Line 349)

13. Line 306-308. The sentence “This is also confirmed by the significant correlations of $\sum_{24}$PAHs with the biomass burning tracer, levoglucosan, the coal combustion tracer, picene, and the vehicle exhaust tracer, hopanes at most sites.” should be re-phrased to “This is also confirmed by the significant correlations of $\sum_{24}$ PAHs with the typical tracers of biomass burning (levoglucosan), coal combustion (picene) and vehicle exhaust (hopanes)”.

Reply: Revised as suggested. (Line 356-357)

14. Line 314. Replace “biomass tracer” to “biomass burning tracer”.

Reply: Revised as suggested. (Line 367)

15. Line 338-340. Provide the full words for the abbreviation “SCE”.

Reply: Revised as suggested. (Line 391-392)

16. Figure 8. Please illustrate in the figure caption that the black dot-line represents the ILCR.

Reply: Revised as suggested.

17. Table S4. Please add a line in the table to distinguish the sites in the northern China and the southern China.

Reply: We revised Table S4 to distinguish the sites in the northern China and the southern China.

18. Figure S11. Please add legend in the figure.

Reply: Revised as suggested.

Referee comment to acp-2020-576-RC2

This work conducted comprehensive field measurements of PAHs in fine particles at 12 sites in China for one year to investigate the chemical compositions, size-distributions, spatiotemporal variations, as well as the public health risk. In addition, diagnostic ratios and PMF model were applied to quantify the contributions from different sources to PAHs in northern China and southern China, highlighting the significant impacts from coal combustion and biomass burning, especially in winter in northern China. The manuscript is generally well written with clear logic, fluent language, abundant data, and deep analyses. There are some minor comments and suggestions below which are required to address before being accepted.

Specific comments:

1. Figure 1, keep the longitude and latitude of the map in same scale. If possible, try to use the coordinate of latitude and longitude instead of Cartesian coordinate when drawing the whole map of China.

Reply: Thank you for your suggestion. We add the coordinate of latitude and longitude in Figure 1.

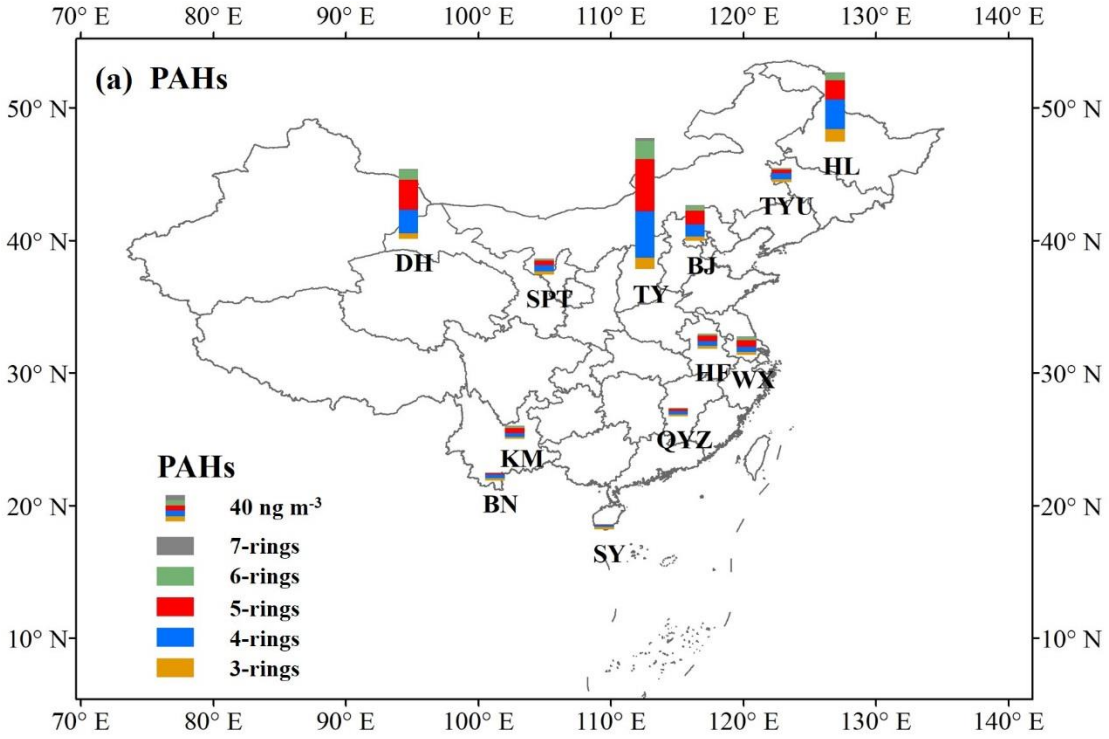

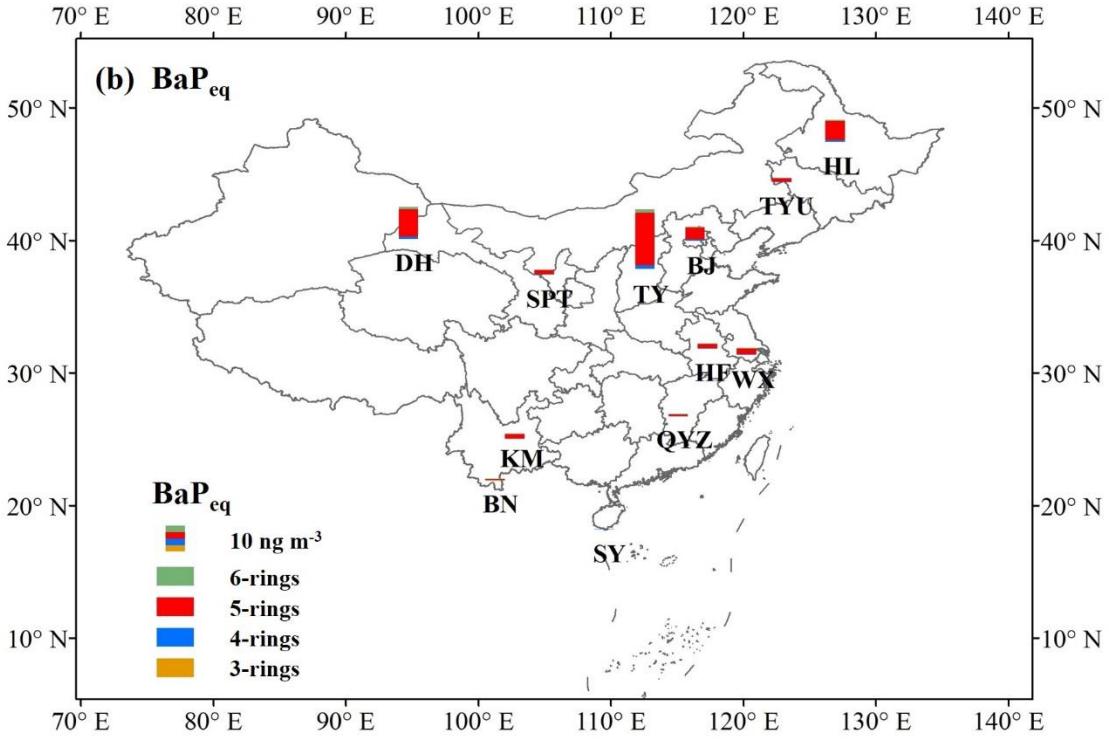

Figure 1 Annual averages of $\sum_{24}$ PAHs (a) and BaP_{eq} (b) at 12 sites in China.

2. Line 91, delete the extra word “in”.

Reply: Revised as suggested. (Line 96) (The line numbers here refers to the ‘tracking changes’

file).

3. Line 134-135 and Figure 8, state the basis of season division. Why four months are included in summer but only two in autumn?

Reply: Season division is based on consistent annual changes in the weather. According to the meteorological definition, each season lasts three months that spring runs from March to May, summer runs from June to August, fall (autumn) runs from September to November, and winter runs from December to February. In the revised manuscript, we state the basis of season division in the caption and revise the figure. Figure 2 here was Figure 8 in the revised manuscript.

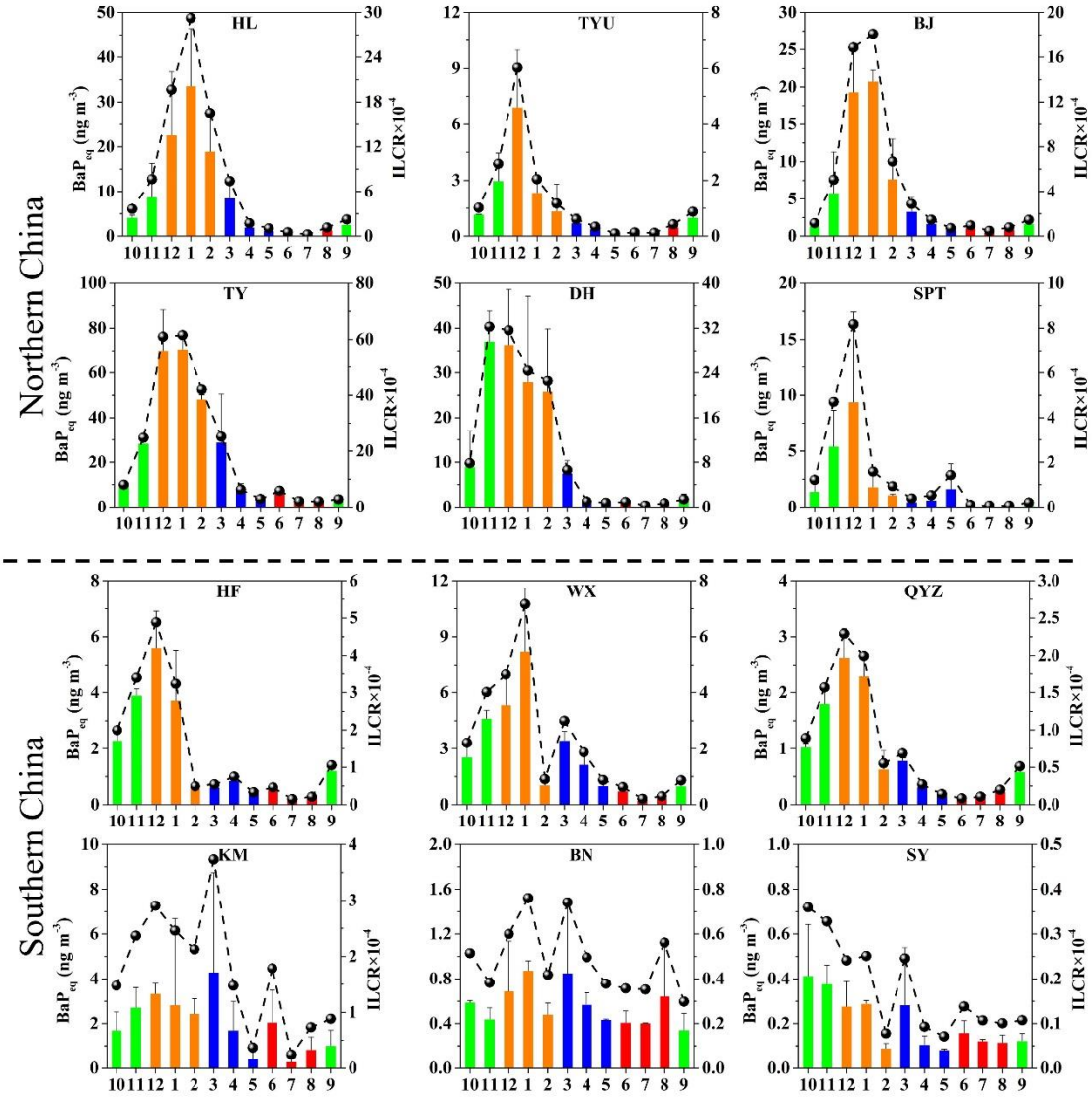

Figure 2 Monthly variations of BaP_{eq} and ILCR at sites in the northern China and the southern

China. The green, yellow, blue and red bars represent BaP_{eq} in fall (October-November, 2012 and September, 2013), winter (December 2012-February 2013), spring (March-May, 2013), and summer (June-August, 2013), respectively. The black dot represented the ILCR.

4. Line 149-153, point out the amount of the added internal standards and the specific extraction method.

Reply: Thank you for your suggestion. In this study, we added 400 μL of internal standards into each sample. The extraction method is ultrasonic solvent extraction.

"Before ultrasonic solvent extraction, 400 μL of isotope-labeled mixture compounds (tetracosane-d50, napthalene-d8, acenaphthene-d10, phenanthrene-d10, chrysene-d12, perylene-d12 and levoglucosan-^{13}C6) were spiked into the samples as internal standards." (Line 161-164)

5. Line 233-235 and 239-241, why most of the PAHs existed in ultrafine particles and the fractions in ultrafine particles varied with seasons? Is this related to the emission sources?

Reply: Yes, it should be related to the emission sources of PAHs. Atmospheric PAHs are mainly derived from combustion sources. As Shen et al. (2013) reported (see Figure 3 below), PAHs emitted form biomass burning and coal combustion enriched in ultrafine particles (<1.1 μm). Moreover, coal combustion witnessed more enrichment of PAHs in ultrafine particles than biomass burning.

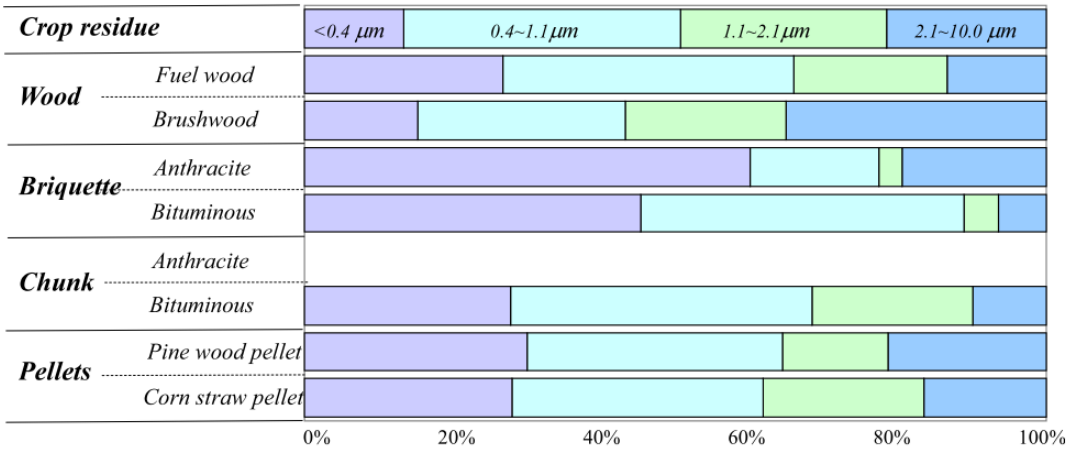

Figure 3 Size distribution of particle-phase PAHs in emissions for different fuels (Shen et al., 2013)

Our PMF results showed an apparently seasonal trend of PAHs sources. For instant, at the DH site, the contributions of coal combustion kept decreasing from winter to summer, while biomass burning kept increasing (Figure 4a). Such a change in PAH sources indeed resulted in the seasonal variations of PAH fractions in ultrafine particles that the mass fractions of Σ_{24}PAHs in $PM_{1.1}$ were the highest during fall to winter and the lowest during summer (Figure 4b).

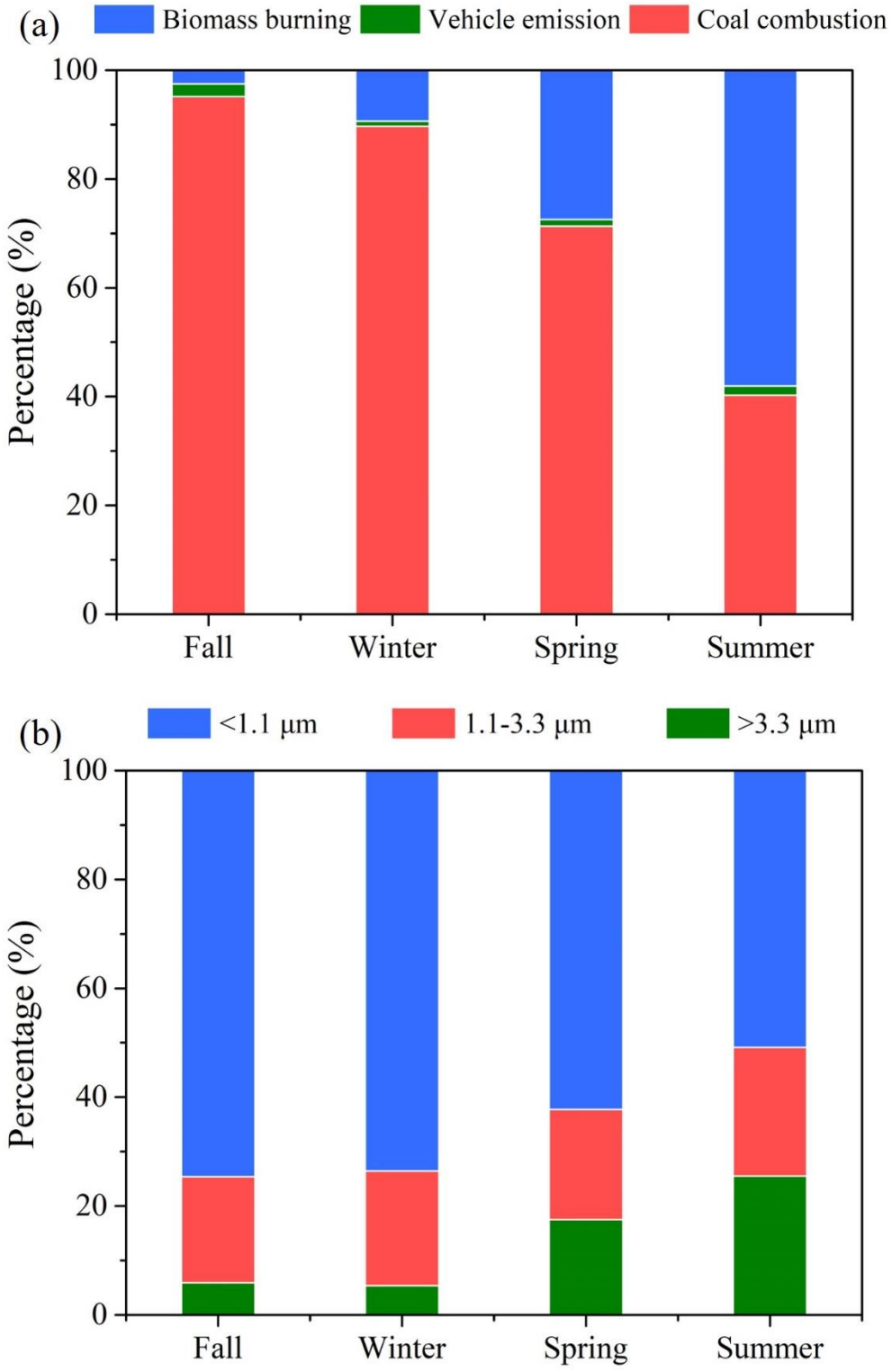

Figure 4 Seasonal variations of PAHs source contributions at DH (a); size distribution of $\sum_{24}$PAHs in different season at DH.

Shen, G.F., Tao, S., Chen, Y.C., Zhang, Y.Y., Wei, S.Y., Xue, M., Wang, B., Wang, R., Lu, Y., Li, W., Shen, H.Z., Huang, Y., Chen, H., 2013. Emission characteristics for polycyclic aromatic hydrocarbons from solid fuels burned in domestic stoves in rural China. Environ. Sci. Technol. 47, 14485-14494.

6. Section 3.3, is there any difference in the sources and contributions among urban, sub-urban and rural sites?

Reply: Figure 5 and Figure 6 show the difference of $\sum_{24}$PAHs and BaP_{eq} sources at urban, sub-urban and rural sites, respectively. At urban and sub-urban sites, coal combustion was the largest source of $\sum_{24}$PAHs, followed by biomass burning and vehicle emission, while at remote sites the contributions of coal combustion and biomass burning were comparable and vehicle emission had minor contributions. Coal combustion was the predominated source of BaP_{eq}, and its contribution at urban sites were larger than those at sub-urban and remote sites.

In the revised manuscript, we add more discussion on the difference in the $\sum_{24}$PAH and BaP_{eq} sources among urban, sub-urban and rural sites in Line 410-415 and Line 426-428. Figure 5 and Figure 6 was added in the revised manuscript as Figure 7b and Figure 7e.

"At urban and sub-urban sites coal combustion was the largest source of $\sum_{24}$PAHs (70.4 ng m^{-3}, 85.1% and 30.5 ng m^{-3}, 63.5%), followed by biomass burning (10.1 ng m^{-3}, 12.2% and 16.3 ng m^{-3}, 33.9%) and vehicle emission (2.2 ng m^{-3}, 2.6% and 1.2 ng m-3, 2.5%), while at remote sites the contributions of coal combustion (9.1 ng m^{-3}, 50.6%) and biomass burning (7.8 ng m^{-3}, 43.7%) were comparable and vehicle emission (1.0 ng m^{-3}, 5.7%) had minor contributions (Figure 5) (Line 410-415). Coal combustion was the predominated source of BaP_{eq}, and its

contribution at urban sites (8.3 ng m^{-3} and 96.4%) were larger than those at sub-urban (3.3 ng m^{-3} and 90.8%) and remote (1.0 ng m^{-3} and 82.5%) sites. (Figure 6) (Line 426-428)

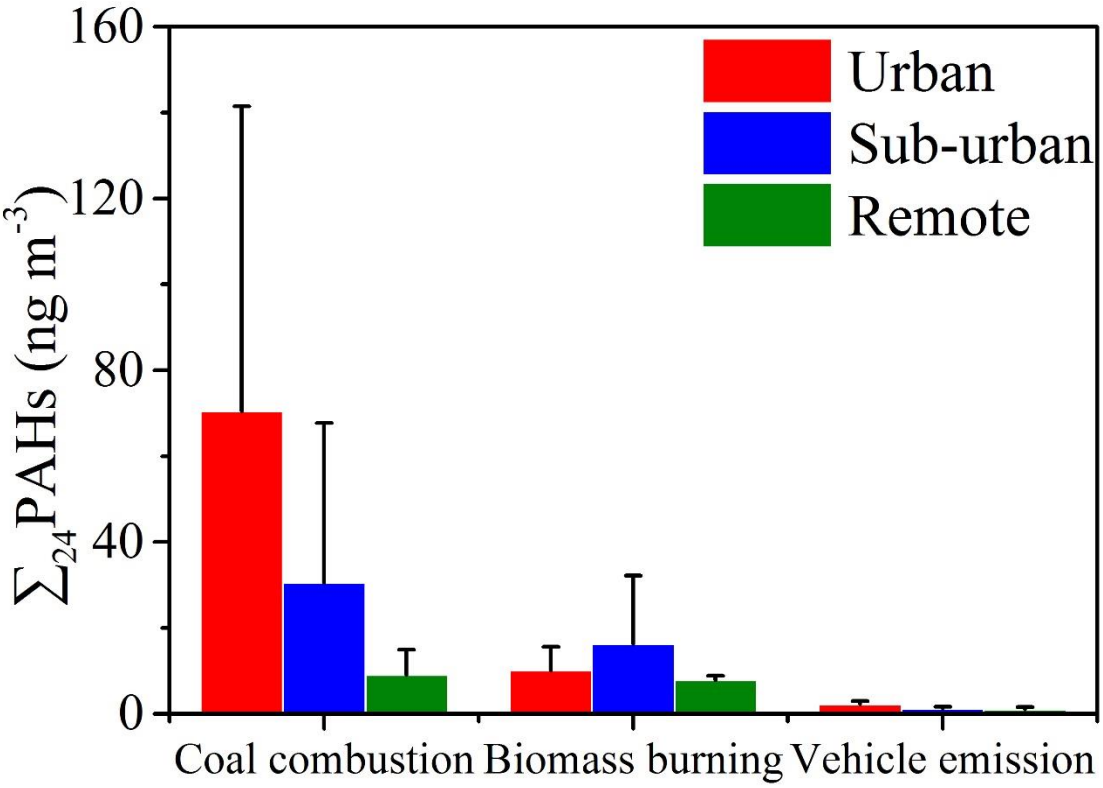

Figure 5 Difference of $\sum_{24}$PAHs sources at urban, sub-urban and remote sites.

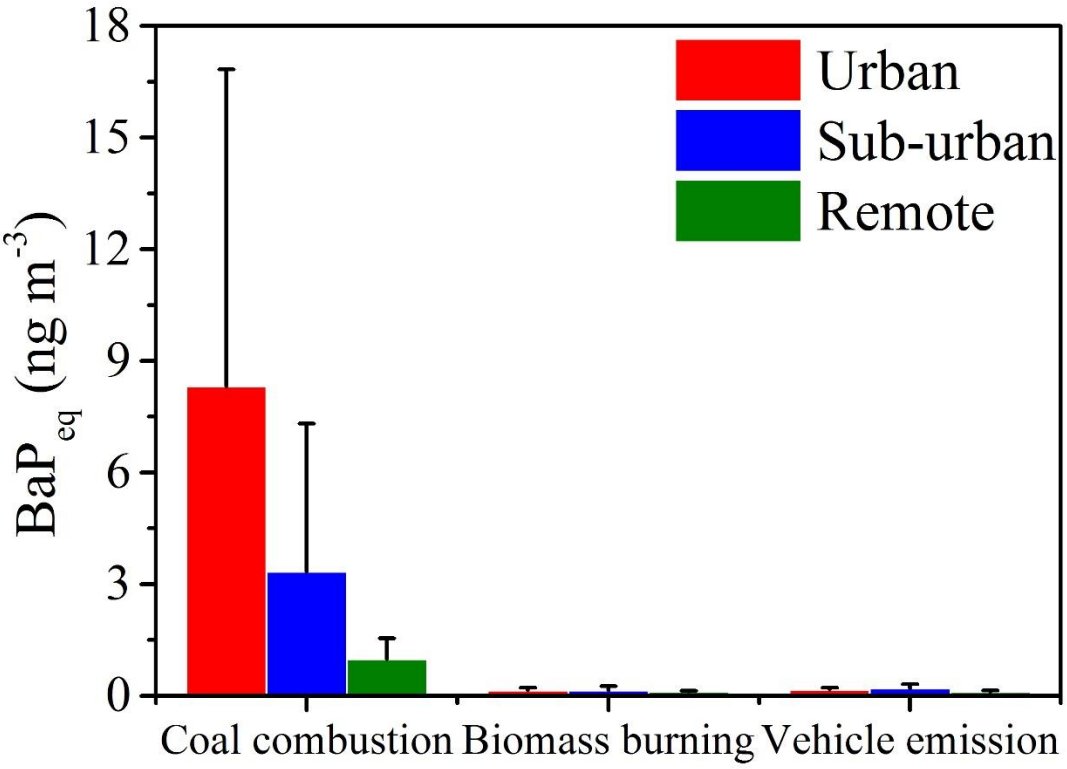

Figure 6 Difference of BaP_{eq} sources at urban, sub-urban and remote sites.

7. Line 336-340, the energy consumption data in 2008 from the Statistical Yearbook are not suitable for comparison. The data in 2013 can be used here.

Reply: Thank you for your suggestion. The data in 2013 from the Statistical Yearbook was used in the revised manuscript. (see below)

"As China statistics yearbook recorded (http://www.stats.gov.cn/english/Statisticaldata/AnnualData/), coal was the dominant fuel in China, accounting for 70.6% (24.1×10^8 tons of Standard Coal Equivalent, SCE) of total primary energy consumption (34.1×10^8 tons of SCE) in 2012, followed by crude oil 19.9% (6.7×10^8 tons of SCE) and other types of energy 9.5%, including biofuel, natural gas, hydro power, nuclear power and other power (3.2×10^8 tons of SCE)." (Line 390-395)

8. Figure 8, it’s better to remove the repeated ordinate title of the middle graphs.

Reply: Revised as suggested.

Comment on manuscript on acp-2020-576

Overall, this manuscript is short on bright spots and largely repeats known conclusions. The current level does not meet the publication standards of Atmospheric Chemistry and Physics.

I am not sure that using the same sampling and analysis methods to carry out TSP size-grading sampling in northern and southern China can be an advantage of this study. Because the results presented by the authors are comparable to those of other studies, this equivalence, to some extent, may indicate that the measurements are comparable despite the differences in sampling and analysis methods.

Reply: Thank you for your comment. Public concerns on polycyclic aromatic hydrocarbons (PAHs) are mainly due to their carcinogenic potential. As the largest developing country in the world, China is the largest PAHs emitter and has high cancer risks caused by PAHs exposure. PAHs in different size particles have different health impacts. Thus, it is essential to understand size distribution of PAHs levels and sources and discover their difference in health risks among typical regions of China (e.g. north vs. south, urban vs. remote). These results are helpful to provide a basis for PAHs pollution control and health effects reduction in different regions of China. Unfortunately, most previous studies on atmospheric PAHs are undertaken at several sites within a local or regional scale in China. Due to the inconsistency in sampling methods, frequency and duration in these local and regional campaigns, it is difficult to draw a national picture of PAHs pollution in the air of China. To the best of our knowledge, our national observation is one of the first studies to acquire comprehensive information concerning spatiotemporal characteristics, source apportionment and health risks of size-segregated PAHs over a large national scale.

Based on our observation, we find that PAHs and BaP_{eq} are dominated in $PM_{1.1}$ at all sites,

indicating that high carcinogenicity of PAHs is accompanied with ultrafine particles. Nationwide increases in both PAH levels and inhalation cancer risks occur in winter, probably due to the unfavorable meteorological conditions and enhanced emissions of coal combustion and biomass burning. Moreover, in the revised manuscript, we add more discussion focusing on PAHs and BaP_{eq} sources in different size particles and among urban, sub-urban and remote sites. We find that coal combustion is the major source of BaP_{eq} in all size particles at most monitoring sites. We believe that these findings provide insights into PAHs pollution and its potential effect on public health in China. Thus, this information is helpful to provide a basis for PAHs pollution control and health effects reduction in different regions of China.

The correlation analysis between PAH concentration and meteorological parameters in this manuscript might be reconsidered. The meteorological parameters, T, SR, and BHL, were low in winter and high in summer, while the concentration of PAHs changed in the opposite way. This difference constitutes an inverse correlation between these meteorological parameters and the concentration of PAHs. Therefore, the authors' emphasis on the worsened PAH pollution in winter caused by adverse meteorological conditions is lack of argument. It is suggested to analyze the correlation between PAH concentration and meteorological parameters in northern and southern China in each season, and it is better to normalize the concentration at different sites. On the other hand, it is well known that the effect of meteorological conditions on pollutants is nonlinear. If feasible, it is desirable to use a nonlinear model to evaluate and even quantify the effect of meteorological conditions on the concentration of PAHs.

Reply: Thank you for your suggestion. Theoretically, adverse meteorological conditions (low

temperature, solar radiation and boundary layer height, etc.) indeed lead to the increase of particulate PAHs. PAHs are semi-volatile compounds (SVOCs) and can partition between the gas and particle phases. The gas-particle (G/P) partitioning behavior of atmospheric PAHs can be described as equations (1) and (2) (Pankow, 1994).

$$K_{p,OM} = \frac{RT}{10^6 \overline{MW_{OM}} \zeta_{OM} P_L^o} \quad (1)$$

$$P_L^o = P_L^{o,*} \exp[\frac{\Delta H_{vap}^*}{R} (\frac{1}{298.15} - \frac{1}{T})] \quad (2)$$

where $K_{p, OM}$ represents the absorptive G/P partitioning coefficient of individual PAH, R (m^3 Pa/(K/mol)) is the ideal gas constant, T (K) is the ambient temperature. $\overline{MW_{OM}}$ (g/mol) is the mean molecular weight of organic matter (OM) and is assumed to be 200 g/mol (Xie et al., 2014), ζ_{OM} is the scale activity coefficient of each compound in the absorbing phase and is usually assumed to be unity. $P_L^{o,*}$ is the vapor pressure of each PAH at 298.15K and ΔH_{vap}^* is vaporization enthalpy of the liquid at 298.15K. Thus, for a specific PAH in a single OM phase at a fixed relative humidity, the G/P partitioning should be driven by ambient temperature only. As Figure 1 showed, the decrease of ambient temperature can cause the increase of $K_{p, OM}$. This means that the decrease of ambient temperature would result in the increase of individual PAH in the particulate phase assuming a constant total concentration in the air.

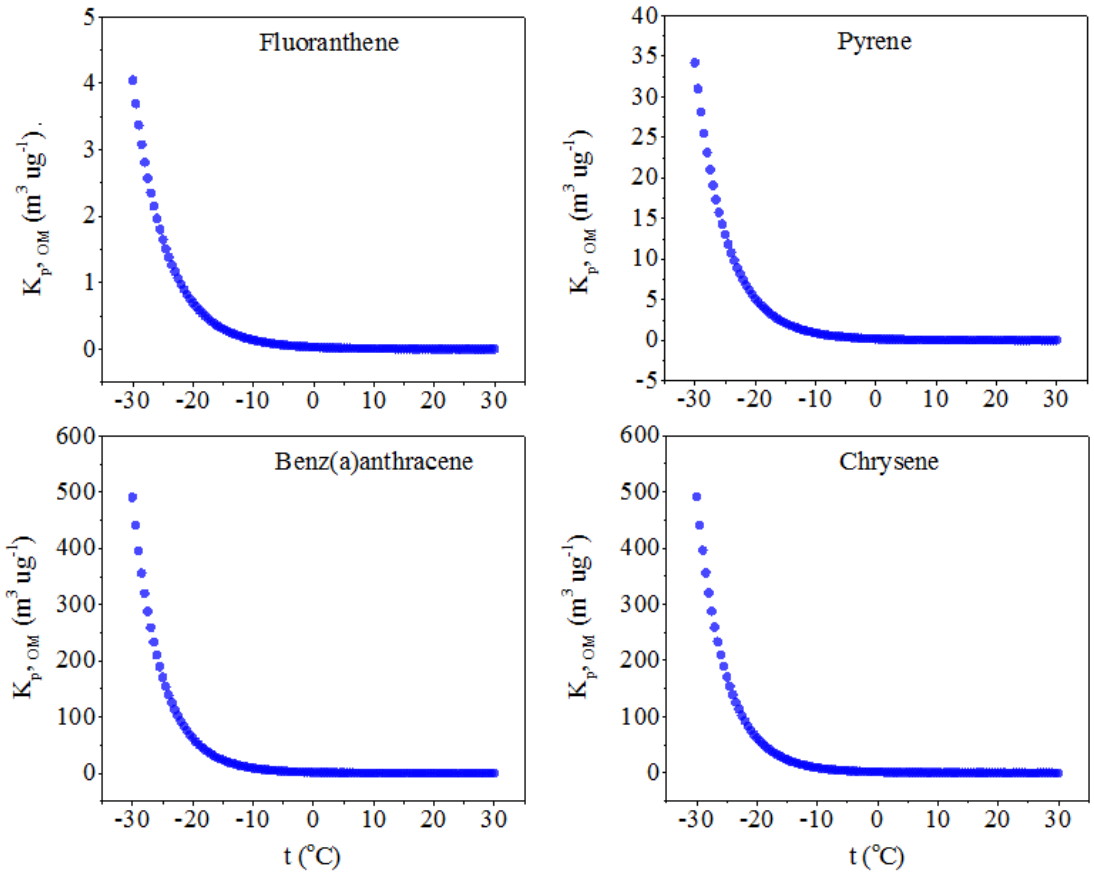

Figure 1 The $K_{p,OM}$ (m^3 ug^{-1}) under different temperature.

In the atmosphere, PAHs removal by OH can be described as:

$$\frac{dC_{PAH}}{dt} = -k * [OH] * C_{PAH} \qquad (3)$$

where k is the rate constant for the reaction of a PAH with OH radical, C_{PAH} is the concentration of individual PAH in the air. Solar radiation (SR) directly affects photochemistry in the air. As Figure 2 showed, solar radiation values during our campaign positively correlated with the concentrations of hydroxyl radical [OH] which were estimated based on the empirical equation (4) (Ehhalt and Rohrer, 2000). Thus, the decrease of SR can indeed lower [OH] and accumulate PAHs in the air, resulting in the increase of PAHs concentrations.

$$[\mathrm{OH}] = \mathrm{a}(JO^1D)^{\alpha}(JNO_2{}^{\beta})\frac{bNO_2+1}{cNO_2{}^2+dNO_2+1} \qquad (4)$$

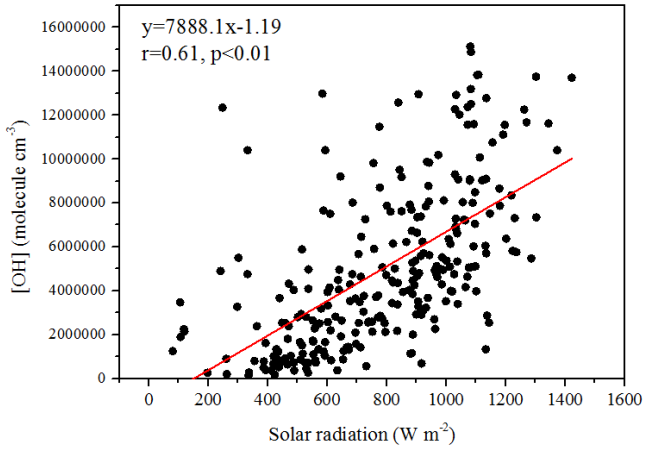

Figure 2 Correlation between OH concentration and solar radiation.

For the influence of boundary layer, low height of boundary layer can inhibit the vertical diffusion of PAHs, which leads to PAHs accumulation and increased concentrations.

We agree with the reviewer that the effect of meteorological conditions on pollutants is nonlinear. It is better to use a nonlinear model to evaluate the effect, which is out of the scope of the current study. At least above discussion illustrates theoretical inverse relationships between these meteorological parameters (temperature, solar radiation and boundary layer height) and the concentration of particulate-bound PAHs.

As suggested by the reviewer, we try to analyze the correlations between PAH concentrations and meteorological parameters in each season. Unfortunately there is only six samples in each season at a site. Instead, we divide the one-year data into warm and cold seasons based on the ambient temperature. As Figure 3 showed, at most sites in the northern and southern China, PAHs negatively correlated with temperature (T), boundary layer height (BLH) and solar radiation (SR) in both cold ($T < 10\ ^\circ C$) and warm ($T > 10\ ^\circ C$) seasons. Thus, coupled with above theoretical discussion, we believe our correlation analysis does reflect the effect of meteorological parameter on PAH concentrations.

In the revised manuscript, we add more discussion about the effect of meteorological parameter on PAH concentrations in Line 297-305 and Line 318-323. And Figure 3 was added in supporting information file and the revised manuscript as Figure S10. The detail theoretical discussion information had been added to the supporting information as Text S1 (The line numbers here refers to the 'tracking changes' file)

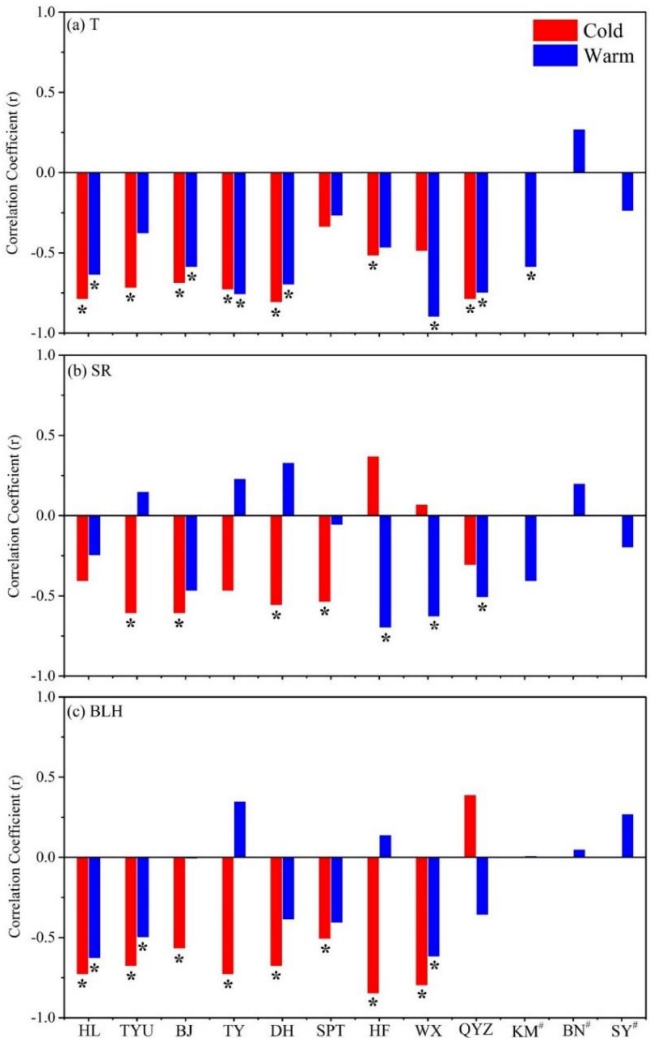

Figure 3 Correlation coefficient (r) of PAHs with T (a), SR (b) and BHL (c) at 12 sites in cold and warm season.

*: $p<0.05$

#: the ambient temperature in KM, BN and SY are all exceed ten degree, there are no cold season in these three sampling sites.

In addition, the source analysis of PAHs does not seem to be in-depth. It is expected to link the source contribution to the health risks of a specific PAH. This relation will improve the understanding of the impact of changes in emission sources on the composition and health risks of PAHs, which will be more conducive to the development of effective local control measures.

Reply: Thank you for your suggestion. BaP carcinogenic equivalent concentration (BaP_{eq}) is widely used to evaluate the health risks of PAHs. In the revised manuscript, we add more discussion focusing on source apportionment of BaP_{eq} as well as $\sum_{24}$PAHs in different size particles and urban, sub-urban and remote sites. To the best of our knowledge, this is one of the first studies to acquire comprehensive information concerning observation-based source apportionment of size-segregated PAHs and BaP_{eq} over a large national scale.

Figure 4 show source apportionment of $\sum_{24}$PAHs in different regions (a), sampling sites (b) and size particles (c). In the northern China, coal combustion was the major source of atmospheric PAHs (73.6 ng m^{-3}, 84.2% of $\sum_{24}$PAHs), followed by biomass burning (11.8 ng m^{-3} and 13.5%) and vehicle exhaust (2.0 ng m^{-3} and 2.3%). In the southern China, coal combustion (9.6 ng m^{-3} and 54.8%) and biomass burning (6.8 ng m^{-3} and 39.0%) were the major contributors, followed by vehicle exhaust (1.1 ng m^{-3} and 6.2%) (Figure 4a). At urban and sub-urban sites, coal combustion was the largest source of $\sum_{24}$PAHs (70.4 ng m^{-3}, 85.1% and 30.5 ng m^{-3}, 63.5%), followed by biomass burning (10.1 ng m^{-3}, 12.2% and 16.3 ng m^{-3}, 33.9%) and vehicle emission (2.2 ng m^{-3}, 2.6% and 1.2 ng m^{-3}, 2.5%), while at remote sites the contributions of coal combustion (9.1 ng m^{-3}, 50.6%) and biomass burning (7.8 ng m^{-3}, 43.7%) were comparable and vehicle emission (1.0 ng m^{-3}, 5.7%) had minor contributions. The major sources of $\sum_{24}$PAHs varied among different size particles in the northern and southern China (Figure 4c).

For $PM_{>3.3}$-bound PAHs, the contributions of coal combustion (50.3%) and biomass burning (48.4%) were comparable in the northern China, while biomass burning (71.0%) was the largest source in the southern China. For $PM_{1.1\text{-}3.3}$-bound PAHs, coal combustion (66.7%) was the dominated source in the northern China, whereas the percentage of biomass burning (53.7%) was larger than that of coal combustion (40.4%) in the southern China. For $PM_{1.1}$-bound PAHs, coal combustion was the dominated source in the northern (66.6%) and southern (59.3%) China.

Figure 4 shows source apportionment of BaP_{eq} in different regions (d), sampling sites (e) and size particles (f). Unlike $\sum_{24}$PAHs, coal combustion was the predominant source of BaP_{eq} in the northern (8.1 ng m^{-3} and 95.7%) and the southern (1.1 ng m^{-3} and 84.7%) China. The contributions of coal contribution at urban sites (8.3 ng m^{-3} and 96.4%) were larger than those at sub-urban (3.3 ng m^{-3} and 90.8%) and remote (1.0 ng m^{-3} and 82.5%) sites. Coal combustion was the dominate source in different size particles. And its contributions to $PM_{>3.3}$, $PM_{1.1\text{-}3.3}$ and $PM_{1.1}$-bound PAHs in the northern China (87.3%, 95.6% and 96.9%) were all larger than those in the southern China (76.8%, 87.3% and 88.2%).

All these discussion has been added to the revised manuscript in Line 381-386 and Line 409-430. And Figure 4 was added in the revised manuscript as Figure 7. We believe these findings provide insights into the linkage between the source contributions to the health risks of atmospheric PAHs and improve the understanding of the impact of changes in emission sources on the compositions and health risks of PAHs.

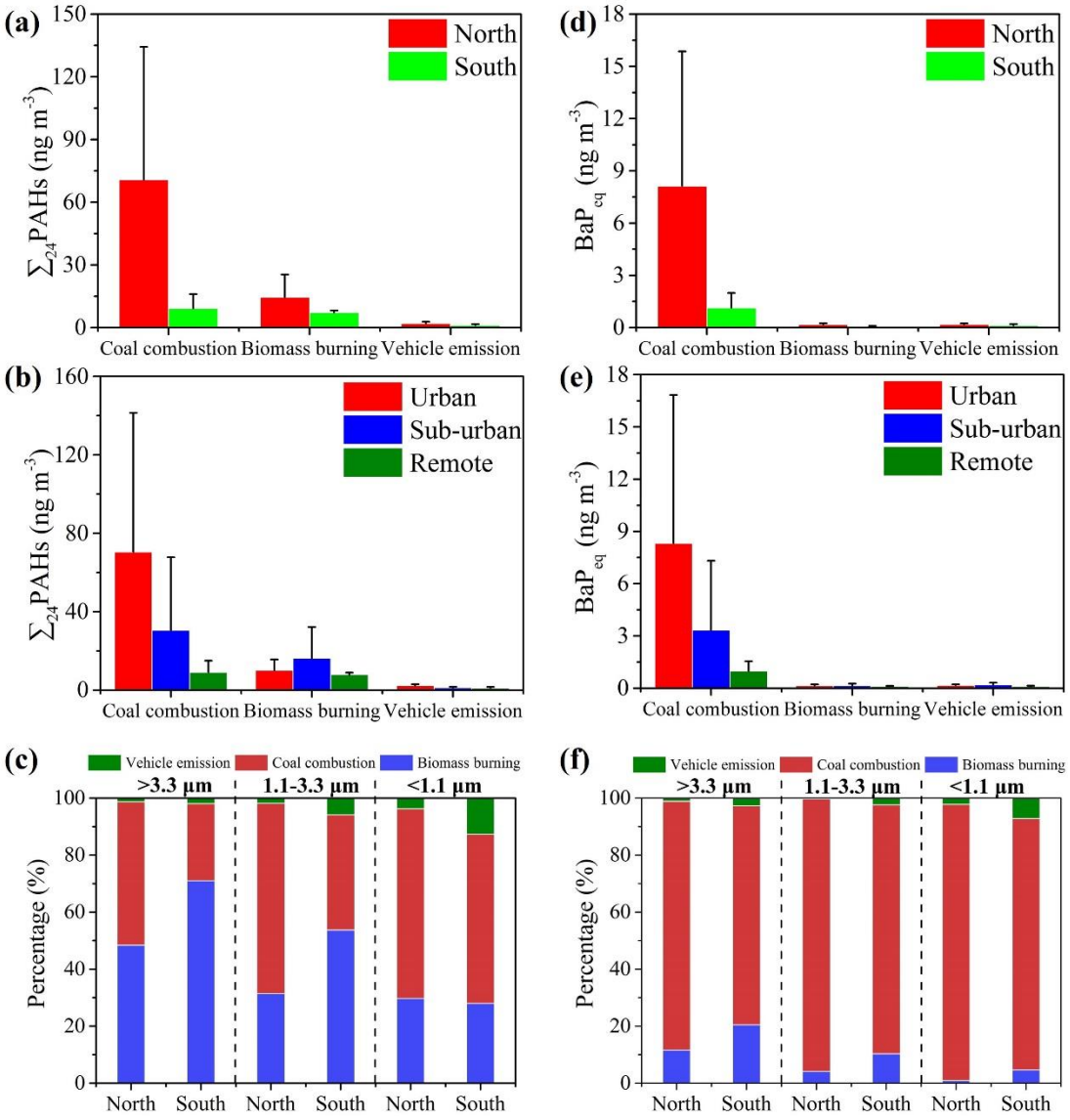

Figure 4 Source apportionment of $\sum_{24}$ PAHs and BaP$_{eq}$ in different regions (a, c), sampling sites (b, d) and size particles (c, f).

References

Ehhalt, D.H., Rohrer, F., 2000. Dependence of the OH concentration on solar UV. J. Geophys. Res.-Atmos. 105, 3565-3571.

Pankow, J.F., 1994. An absorption model of gas/particle partitioning of organic compounds in the atmosphere. Atmos. Environ. 28, 185-188.

Xie, M., Hannigan, M.P., Barsanti, K.C., 2014. Gas/particle partitioning of n-alkanes, PAHs and oxygenated PAHs in urban Denver. Atmos. Environ. 95, 355-362.

Nationwide increase of polycyclic aromatic hydrocarbons in ultrafine particles during winter over China

Qingqing Yu[a], Xiang Ding[a,d,*], Quanfu He[a], Weiqiang Yang[e], Ming Zhu[a,b], Sheng Li[a,b], Runqi Zhang[a,b], Ruqin Shen[a], Yanli Zhang[a,c,d], Xinhui Bi [a,d], Yuesi Wang[c,f], Ping'an Peng[a,d], Xinming Wang[a,b,c,d,*]

[a]State Key Laboratory of Organic Geochemistry and Guangdong Key Laboratory of Environmental Protection and Resources Utilization, Guangzhou Institute of Geochemistry, Chinese Academy of Sciences, Guangzhou 510640, China

[b]University of Chinese Academy of Sciences, Beijing 100049, China

[c]Center for Excellence in Regional Atmospheric Environment, Institute of Urban Environment, Chinese Academy of Sciences, Xiamen 361021, China

[d]Guangdong-Hong Kong-Macao Joint Laboratory for Environmental Pollution and Control, Guangzhou Institute of Geochemistry, Chinese Academy of Science, Guangzhou 510640, China

[e]Guangdong Provincial Academy of Environmental Science, Guangzhou 510045, China

[f]State Key Laboratory of Atmospheric Boundary Layer Physics and Atmospheric Chemistry, Institute of Atmospheric Physics, Chinese Academy of Sciences, Beijing 100029, China

*corresponding author:

Dr. Xinming Wang and Dr. Xiang Ding

State Key Laboratory of Organic Geochemistry Guangzhou Institute of Geochemistry, Chinese Academy of Sciences, 511 Kehua Rd, Tianhe, Guangzhou, 510640, China.

Email addresses: wangxm@gig.ac.cn and xiangd@gig.ac.cn

Abstract

Polycyclic aromatic hydrocarbons (PAHs) are toxic compounds in the atmosphere and have adverse effects on public health, especially through the inhalation of particulate matter (PM). At present, there are limited understandings in size distribution of particulate-bound PAHs and its health risk on a continental scale. In this study, we carried out simultaneously ~~a one-year~~ PM campaign from October, 2012 to September, 2013 at 12 sampling sites including urban, sub-urban and remote sites in different regions of China. ~~and simultaneously measured~~ Ssize-segregated PAHs and typical tracer of coal combustion (picene), biomass burning tracer (levoglucosan) and vehicle exhaust (hopanes) were measured. ~~at 12 sites across six regions of China.~~ The annual averages of total 24 PAHs ($\sum_{24}$PAHs) and benzo[a]pyrene (BaP) carcinogenic equivalent concentration (BaP_{eq}) ranged from 7.56 to 205 ng m^{-3} with a mean of 53.5 ng m^{-3} and 0.21 to 22.2 ng m^{-3} with a mean of 5.02 ng m^{-3}, respectively. At all the sites, $\sum_{24}$PAHs and BaP_{eq} were dominated in the ultrafine particles with aerodynamic diameter <1.1 μm, followed by those in the size ranges of 1.1-3.3 μm and >3.3 μm. Compared with the southern China, the northern China witnessed much higher $\sum_{24}$PAHs (87.36 ng m^{-3} vs. 17.56 ng m^{-3}), BaP_{eq} (8.48 ng m^{-3} vs. 1.34 ng m^{-3}) and PAHs inhalation cancer risk (7.4×10^{-4} vs. 1.2×10^{-4}). Nationwide increases in both PAH levels and inhalation cancer risk occurred in winter. The unfavorable meteorological conditions and enhanced emissions of coal combustion and biomass burning together led to severe PAHs pollution and high cancer risk in the atmosphere of the northern China, especially during winter. Coal combustion is the major source of BaP_{eq} in all size particles at most sampling sites. Our results suggested that the reduction of coal and

biofuel consumption in the residential sector could be crucial and effective to lower PAH concentrations and its inhalation cancer risk in China.

Key words: Polycyclic aromatic hydrocarbons; ~~inhalation cancer risk;~~ China; inhalation cancer risk; coal combustion; biomass burning

1. Introduction

Ambient particulate matter (PM) pollution has adverse effects on public health. The global deaths caused by exposure to the PM with aerodynamic diameters less than 2.5 μm ($PM_{2.5}$) kept increasing from 1990 and reached 4.2 million in 2015 (Cohen et al., 2017). In China, ambient $PM_{2.5}$ pollution ~~was~~ ranked the fourth leading ~~factor~~ risks for ~~mortality~~ deaths (Yang et al., 2013), and caused 1.7 million premature deaths in 2015 (Song et al., 2017). Adverse health impacts of PM are associated with particle size and chemical components (Chung et al., 2015; Dong et al., 2018). Higher risk of cardiovascular disease was associated with smaller size-fractioned particulate matter, especially $PM_{1.0}$-bound particulate matter (Yin et al., 2020).

Polycyclic aromatic hydrocarbons (PAHs) are a group of organic substances~~compounds~~ composed of two or more~~–~~ aromatic rings~~benzene rings~~. Due to the mutagenic, teratogenic, and carcinogenic properties (Kim et al., 2013), PAHs are one of the most toxic components in PM (Xu et al., 2008). Toxic PAHs usually enrich~~es~~ in fine particles, especially the aerodynamic diameters less than 1.0 μm (Wang et al., 2016; Li et al., 2019) ~~and~~ which can enter the human respiratory system through inhalation (Yu et al., 2015). Exposure to PAHs likely induces DNA damage and raises the risk of gene mutation (Zhang et al., 2012; Lv et al., 2016) and cardiopulmonary mortality (Kuo et al., 2003; John et al., 2009). Previous studies have demonstrated that inhalation exposure to PAHs can cause high risk of lung cancer (Armstrong et al., 2004; Zhang et al., 2009; Shrivastava et al., 2017).

Atmospheric PAHs are mainly emitted from incomplete combustion of fossil fuels and biomasses (Mastral and Callen, 2000). As typical semi-volatile chemicals, PAHs can transport over long distances (Zelenyuk et al., 2012) and have been detected in the global atmosphere (Brown et al., 2013; Garrido et al., 2014; Hong et al., 2016; Liu et al., 2017a; Hayakawa et al.,

2018). Emission inventory indicated that developing countries were the major contributors to global PAHs emission (Zhang and Tao, 2009; Shen et al., 2013a).

As the largest developing country in the world, China has large amounts of PAHs emission and high cancer risk caused by PAHs exposure. The annual emission of 16 USEPA priority PAHs in China sharply increased from 18 Gg in 1980 to 106 Gg in 2007 (Xu et al., 2006; Shen et al., 2013a). China became the largest emitter of PAHs ~~on a global scale~~, accounting for about 20% of the ~~total~~ global PAHs emission during 2007 (Shen et al., 2013a). The excess ~~incremental lifetime~~ lung cancer risk ~~(ILCR)~~ caused by inhalation exposure to ambient PAHs was estimated to be 6.5×10^{-6} in China (Zhang et al., 2009), which was ~~much~~ 5.5 times higher than the acceptable risk level of 1.0×10^{-6} in US (USEPA, 1991). As Hong et al. (2016) estimated, the lifetime excess lung cancer cases caused by exposure to PAHs for China ranged from 27.8-2200 per million people and were higher than other Asia counties.

Moreover, PAHs emission and cancer risk in China have large spatial and seasonal variations. As reported by Tao and coworkers, high emission of PAHs occurred in the North China Plain (Zhang et al., 2007), and the emission in winter was 1.6 times higher than that in summer (Zhang and Tao, 2008). Thus, the lung cancer risk caused by ambient PAH inhalation exposure in the northern China was higher than that in the southern China (Zhang et al. 2009). In addition, through long-range atmospheric transport, PAHs emitted in China could spread to ~~the neighbor countries and regions in Northeast Asia and even reach the western US~~ other regions of the world (Zhang et al., 2011; Inomata et al., 2012).

For more accurate estimation of inhalation exposure to ambient PAHs and its cancer risks in China, it is essential to carry out nationwide campaigns to acquire spatial and seasonal

characteristics of atmospheric PAHs. The data of PAHs in the ambient air are accumulating in China during the past decades. Among these filed studies, most were conducted ~~in~~ in rapidly developing economic regions, including the North China region (Huang et al., 2006; Liu et al., 2007a; Wang et al., 2011; Lin et al., 2015a; Lin et al., 2015b; Tang et al., 2017; Yu et al., 2018), Yangtze River Delta region (Liu et al., 2001; Zhu et al., 2009; Gu et al., 2010; He et al., 2014) and Pearl River Delta region (Bi et al., 2003; Guo et al., 2003; Li et al., 2006; Tan et al., 2006; Duan et al., 2007; Lang et al., 2007; Yang et al., 2010; Gao et al., 2011, 2012, 2013, 2015; Yu et al., 2016), due to large amounts of combustion emission and high density of population in these regions. These studies provided insight into the fate and health risk of airborne PAHs on a local or regional scale. However, due to the inconsistency in sampling methods, frequency and duration in these local and regional campaigns, it is difficult to draw a national picture of PAHs pollution in the air of China.

There are rare dataset discovering nationwide characteristics of airborne PAHs over China. Liu et al. (2007b) reported PAHs in the air of 37 cities across China using passive polyurethane foam (PUF) disks. Wang et al. (2006) and Liu et al., (2017b) determined $PM_{2.5}$-bound PAHs over 14 and 9 Chinese cities, respectively. PAHs in the total suspended particle (TSP) and gas phase were measured over 11 cities in China (Ma et al., 2018; Ma et al., 2020). Besides these important information of PAHs in the bulk PM, it is vital to determine size distribution of PAHs, since the size of particles is directly linked to their potential for causing health problems. On the national scale, at present, there is only one field study available reporting size-segregated atmospheric PAHs at 10 sites (Shen et al., 2019). Therefore, it is essential to carry out large range campaigns coving multiple types of sites across different regions to investigate size

distribution of PAHs levels and sources and discover their difference in health risks among typical regions of China (e.g. north vs. south, urban vs. remote). ~~the distribution and risk of atmospheric PAHs in different size particles over China.~~

In this study, we simultaneously collected filter-based size-fractionated PM samples consecutively at 12 sites for one year. We analyzed chemical compositions of PAHs as well as other organic tracers to characterize the spatiotemporal pattern and size distribution of PAHs over China and to explore the possible sources of PAHs on the national scale. This information is helpful to provide a basis for PAHs pollution control and health effects reduction in different regions of China. ~~formulate effective policies on controlling PAHs pollution in different regions of China.~~

2. Materials and Methods

2.1 Field sampling

The PM samples were collected simultaneously at 12 sampling sites across~~in~~ 6 regions of China, ~~including~~ containing five urban sites, three sub-urban sites and four remote sites (Figure S1 and Table S1 in the supporting information). The Huai River-Qin Mountains Line is the geographical line that divides China into the northern and southern regions. There are central heating systems in winter in some urban areas of the northern China, but not so in the southern China. The 12 sampling sites are Beijing (BJ), Dunhuang (DH), Hefei (HF), Hailun (HL), Kunming (KM), Qianyanzhou (QYZ), Sanya (SY), Shapotou (SPT), Taiyuan (TY), Tongyu (TYU), Wuxi (WX) and Xishuangbanna (BN). According to their locations, 6 of the 12 sites are situated in the northern China, including BJ, DH, ~~Hailun (~~HL~~)~~, ~~Tongyu (TYU~~SPT~~), Beijing (BJ)~~, ~~Taiyuan (~~TY~~) , Dunhuang (DH)~~ and TYU ~~Shapotou (SPT)~~. And the remaining 6 sites are

located in the southern China, including BN, ~~Hefei (~~HF~~)~~, KM, QYZ, SY and WX.~~Wuxi (WX), Qianyanzhou (QYZ), Kunming (KM), Xishuangbanna (BN) and Sanya (SY).~~

Total suspended particles (TSP) were collected using Anderson 9-stage cascade impactors (<0.4, 0.4-0.7, 0.7-1.1, 1.1-2.1, 2.1-3.3, 3.3-4.7, 4.7-5.8, 5.8-9.0, >9.0 μm) at a constant flow of 28.3 L/min. Quartz fiber filters (Whatman, QMA) that were used to collect PM samples were prebaked for 8 h at 450 ℃. At each site, one set of nine size-fractionated PM samples were collected for 48-hr every 2 weeks. 294 sets of field samples and one set of field blanks were collected. Detailed information of the field sampling can be found elsewhere (Ding et al., 2014).

~~A total of 294 sets of field samples were collected from October 2012 to September 2013. Additionally, one set of field blanks were collected at each site in the same way as PM samples for 5 minutes when the sampler was turned off. Detailed information of the field sampling was described elsewhere (Ding et al., 2014).~~According to the meteorological definition, each season lasts three months that spring runs from March to May, summer runs from June to August, fall (autumn) runs from September to November, and winter runs from December to February.

The data of average temperature (T), relative humidity (RH), the maximum solar radiation (SR) during each sampling episode were available in the China Meteorological Data Service Center (http://data.cma.cn/en). And the average boundary layer height (BLH) was calculated using the NOAA's READY Archived Meteorology online calculating program (http://ready.arl.noaa.gov/READYamet.php).

2.2 Chemical analysis

~~Since not all size-fractionated filters had detectable levels of PAHs, e~~Each set of nine filters were combined into three samples with the aerodynamic diameters smaller than 1.1 μm ($PM_{1.1}$),

between 1.1 μm and 3.3 μm ($PM_{1.1\text{-}3.3}$), and large than 3.3 μm ($PM_{>3.3}$), respectively. Before ultrasonic solvent extraction, 400 ul of isotope-labeled mixture compounds (tetracosane-d_{50}, napthalene-d_8, acenaphthene-d_{10}, phenethrene-d_{10}, chrysene-d_{12}, perylene-d_{12} and levoglucosan-$^{13}C_6$) were spiked into the samples as internal standards. Samples were ultrasonic extracted twice with the mixed solvent of dichloride methane / hexane (1:1, v/v), and then twice with the mixed solvent of dichloride methane / methanol (1:1, v/v). The extracts of each sample were filtered, combined, and finally concentrated to about 1 mL. Then the extracts were divided into two aliquots for silylation and methylation, respectively. Detailed ~~information~~ information about the procedures of silylation and methylation ~~can be found~~were introduced elsewhere (Ding et al., 2014; Yu et al., 2016).

The methylated aliquot was analyzed for PAHs and hopanes using a 7890/5975C gas chromatography/mass spectrometer detector (GC/MSD) in the selected ion monitoring (SIM) mode with a 60 m HP-5MS capillary column (0.25 mm, 0.25 μm). The GC temperature was initiated at 65 ℃, held for 2 min, and then increased to 300 ℃ at 5 ℃ min^{-1} and held for 40 min. The silylated aliquot was analyzed for levoglucosan using the same GC/MSD in the scan mode with a 30 m HP-5MS capillary column (0.25 mm, 0.25 μm). The GC temperature was initiated at 65 ℃, held for 2 min, and then increased to 290 ℃ at 5 ℃ min^{-1} and held for 20 min. The target compounds were identified by authentic standards and quantified using an internal calibration approach. Table S2 lists the 24 target PAHs and their abbreviations.

2.3 Quality control and quality assurance

Field and laboratory blanks were analyzed in the same manner as the PM samples. The target compounds were not detected or negligible in the blanks. The data reported in this study

were corrected by corresponding field blanks. To test the recovery of the analytical procedure, we analyzed the NIST urban dust Standard Reference Material (SRM 1649b, n=6) in the same manner as the PM samples. Compared with the certified values for PAHs in SRM 1649b, the recoveries were 81.5±1.9%, 66.6±5.4%, 113.6±4.4%, 76.2±2.5%, 100.4±7.9%, 138.3±3.6%, 109.5±14.2%, 125.8±8.8% and 86.4±10.7% for Pyr, Ret, Chr, BbF, BkF, BeP, Per, IcdP and Pic respectively. The data reported in this study were not recovery corrected. The method detection limits (MDLs) of the target compounds ranged from 0.01 to 0.08 ng m^{-3}.

2.4 Positive matrix factorization (PMF) analysis

Positive matrix factorization (PMF)~~A PMF receptor model~~ (USEPA, version PMF 5.0) was employed for source apportionment of PAHs. The model has been widely used to attribute ~~PAH~~ major sources of PAHs (Larsen and Baker, 2003; Belis et al., 2011). In case the observed concentration (*Con*) of a compound was below its MDL, half of the MDL was used as the model input data and the uncertainty (*Unc*) was set as 5/6 of the MDL (Polissar et al., 1998). If the *Con* of a compound was higher than its MDL, *Unc* was calculated as $Unc = [(20\% \times Con)^2 + (MDL)^2]^{1/2}$ (Polissar et al., 1998).

2.5 Exposure assessment

Besides BaP, other PAHs like BaA, BbF, DahA and IcdP are also carcinogenic compounds (IARC, 2001). In order to assess the carcinogenicity of bulk PAHs, the BaP carcinogenic equivalent concentration (BaP_{eq}) was calculated by multiplying the concentrations of PAH individuals (PAH_i) with their toxic equivalency factor (TEF_i) as:

$$BaP_{eq} = \sum_{i=1}^{n} PAH_i \times TEF_i \quad (1)$$

In this study, we adopted the TEFs reported by Nisbet and Lagoy (1992) which were 0.001

for Phe, Flu and Pyr, 0.01 for Ant, Chr and BghiP, 0.1 for BaA, BbF, BkF, BeP, and IcdP, and 1.0 for BaP and DahA. Table S3 lists annual averages of PAH individuals and BaP_{eq} at the 12 sites.

Incremental lifetime lung cancer risk (ILCR) caused by inhalation exposure to PAHs was estimated as:

$$ILCR=BaP_{eq}\times UR_{BaP} \quad (2)$$

where UR_{BaP} is the unit relative risk of BaP. Based on the epidemiological data from studies in coke-oven workers, the lung cancer risk of BaP inhalation was estimated to be 8.7×10^{-5} per ng m^{-3} (WHO, 2000). Thus, we used a UR_{BaP} value of 8.7×10^{-5} per ng/m^3 in this study.

3. Results and discussion

3.1 General marks

Annual averages of the total 24 PAHs ($\sum_{24}$PAHs) in TSP (sum of three PM size ranges) ranged from 7.56 to 205 ng m^{-3} (Figure 1a) among the 12 sampling sites with a mean of 53.5 ng m^{-3}. The highest concentration of $\sum_{24}$PAHs was observed at TY and the lowest level occurred at SY (Figure 1a). Compared with the data in other large scale observations (Table 1), atmospheric concentrations of PAHs measured at the 12 sites in this study were comparable with previously reported values in China in 2013-2014 (Liu et al., 2017b; Shen et al., 2019) and U.S. (Liu et al., 2017a), lower than those measured in China in 2003 and 2008-2009 (Wang et al., 2006; Ma et al., 2018), but higher than those over Great Lakes (Sun et al., 2006), Europe (Jaward et al., 2004), Japan (Hayakawa et al., 2018) and some Asian countries (Hong et al., 2016). Figure 1a also presents the compositions of PAHs. Apparently, 4- and 5-rings PAHs were the majority in $\sum_{24}$PAHs with the mass shares of 36.8±5.6% and 31.4±9.6%, respectively,

followed by the PAHs with 3-rings (19.2±9.4%), 6-rings (11.3±3.8%), and 7-rings (1.3±0.6%). The concentrations of $\sum_{24}$PAHs at urban sites (82.7 ng m^{-3}) were significant higher ($p<0.05$) than those at sub-urban (48.0 ng m^{-3}) and remote sites (18.0 ng m^{-3}) (Figure S2).

Annual averages of BaP in TSP among the 12 sites were in the range of 0.09 to 11.0 ng m^{-3} with a mean of 2.58 ng m^{-3}. The highest level of atmospheric BaP occurred at TY and the lowest existed at SY. The BaP values at five sites (WX, BJ, HL, DH and TY) exceeded the national standard of annual atmospheric BaP (1.0 ng m^{-1}) by factors of 1.2 to 11.0. For BaP_{eq}, annual averages ranged from 0.21 to 22.2 ng m^{-3} with the predominant contribution from 5-rings PAHs~~Annual averages of BaP_{eq} in TSP were in the range of 0.21 to 22.2 ng m^{-3}~~ (Figure 1b)~~ with a mean of 5.02 ng m^{-3}. The highest BaP_{eq} occurred in TY and the lowest existed in SY. And 5-rings PAHs contributed most to BaP_{eq} at all sites. In China, the national standard value of annual atmospheric BaP is 1.0 ng m^{-1m-3}. Among the 12 sites, only three sites (QYZ, BN and SY) had the BaP_{eq} levels met the national standard. The BaP_{eq} values at the rest sites exceeded the national standard by factors of 1.5 to 22.~~ ILCR caused by inhalation exposure to PAHs ranged from 1.8×10^{-5} (SY) -1.9×10^{-3} (TY) among the 12 sites in China (Figure ~~S2~~S3), which were much higher than the acceptable risk level of 1.0×10^{-6} in US (USEPA, 1991). All these demonstrated that China faced severe PAHs pollution and high health risk (Zhang et al., 2009; Shrivastava et al., 2017). And BeP_{eq} (Figure S4) and ILCR (Figure S5) were both the highest at urban sites. All these indicated that people in urban regions of China were faced with higher exposure risk of PAHs pollution as compared to those in rural and remote areas. Figure S6 exhibits that 4- and 5-rings PAHs are the majority in $\sum_{24}$PAHs at urban, sub-urban and remote sites, which totally accounted 72.2%, 63.8% and 66.6% of the total amounts in TSP,

249 respectively. The percentage of 5-rings PAHs dominates at urban sites, and 4-rings PAHs makes
250 the largest proportion at sub-urban and remote sites (Figure S6).

251 **3.2 Enrichment of PAHs in $PM_{1.1}$**

252 Figure 2 presents the size distribution of PAHs and BaP_{eq} at the 12 sites in China. Both
253 $\sum_{24}$PAHs and BaP_{eq} were concentrated in $PM_{1.1}$, accounting for 44.6-71.3% and 56.7-79.3% of
254 the total amounts in TSP, respectively. And BaP_{eq} had more enrichment in $PM_{1.1}$ than $\sum_{24}$PAHs.
255 The mass fractions of $\sum_{24}$PAHs and BaP_{eq} in $PM_{1.1\text{-}3.3}$ were 20.6-39.5% and 16.1-38.3%. The
256 coarse particles ($PM_{>3.3}$) had the lowest loadings of $\sum_{24}$PAHs (7.2-23.4%) and BaP_{eq} (3.0-
257 12.9%). Thus, our observations indicated that PAHs in the ultrafine particles ($PM_{1.1}$) contributed
258 most health risk of PAHs in TSP over China. A previous study at three sites in East Asia found
259 that size distribution of PAHs was unimodal and peaked at 0.7-1.1 μm size (Wang et al., 2009).
260 A recent study at 10 sites of China also found that PAHs were concentrated in $PM_{1.1}$ (Shen et
261 al., 2019). Based on the observation at one site in the Fenhe Plain, northern China, Li et al.
262 (2019) pointed out that PAHs in the particles with the aerodynamic diameters <0.95 μm
263 contributed more than 60% to the total cancer risk of PAHs in PM_{10}. All these results
264 demonstrate that high carcinogenicity of PAHs is accompanied with ultrafine particles,
265 probably because small particles are apt to invade the blood vessels and cause DNA damage.
266 Thus, further studies should put more attentions on PAHs pollution in ultrafine particles.

267 Figure ~~S3~~ S7 and Figure ~~S4~~ S8 show seasonal variations in size distribution of $\sum_{24}$PAHs
268 and BaP_{eq}, respectively. $\sum_{24}$PAHs and BaP_{eq} were enriched in $PM_{1.1}$ throughout the year at all
269 sites. The mass fractions of $\sum_{24}$PAHs and BaP_{eq} in $PM_{1.1}$ were the highest during fall to winter
270 (up to 74.6% and 79.7% at the DH site), and the lowest during summer (down to 39.2% and

50.7% at the BN site). It should be related to the emission sources of PAHs. Atmospheric PAHs are mainly derived from combustion sources. As Shen et al. (2013b) reported, PAHs emitted form biomass burning and coal combustion enriched in ultrafine particles (<1.1 μm). Moreover, coal combustion witnessed more enrichment of PAHs in ultrafine particles than biomass burning. Figure ~~S5~~ S9 presents monthly variations in size distribution of PAHs with different number of rings. The mass shares of 3-rings PAHs in $PM_{1.1}$ (39.2%), $PM_{1.1\text{-}3.3}$ (32.0%) and $PM_{>3.3}$ (28.9%) were comparable. And the highest loading of 3-rings PAHs in $PM_{1.1}$ was observed in December 2012. The mass fractions of 4-ring PAHs in $PM_{1.1}$ were the highest in December 2012 (58.4%) and the lowest in July 2013 (39.5%). The higher molecular weight PAHs (5-7 rings PAHs) were enriched in $PM_{1.1}$ throughout the year.

3.3 High levels of atmospheric PAHs in the northern China

Figure 3 shows the differences of atmospheric PAHs between the northern China (BJ, DH, HL, SPT, TY and TYU~~HL, TYU, BJ, TY, DH and SPT~~) and southern China (BN, HF, KM, QYZ, SY and WX~~HF, WX, QYZ, KM, BN and SY~~). $\sum_{24}$PAHs in the northern China was higher than that in the southern China by a factor of 5.0 (Figure 3a). The concentrations of PAHs with different ring number were all higher in the northern China than those in the southern China, especially for the 4-7 rings PAHs. Moreover, BaP、BaP_{eq} and ILCR in the northern China were 5.8, 5.3 and 5.3 times higher than those in the southern China (Figure 3b). The higher concentrations of PAHs in the air of the northern China than the southern China were also reported in previous field studies (Liu et al., 2017b; Ma et al., 2018; Shen et al., 2019). Based on the emission inventories and model results, previous studies predicted that PAHs concentrations, BaP levels and lung cancer risk of exposure to ambient PAHs in the northern

China were all higher than those in the southern China (Xu et al., 2006; Zhang et al., 2007; Zhang and Tao, 2009; Zhu et al., 2015). All these indicated much higher PAHs pollution and health risk in the northern China.

The northern-high feature of atmospheric PAHs should be determined by the meteorological conditions and source emissions. Theoretical relationship between meteorological parameters (temperature, solar radiation and boundary layer height) and the concentration of particulate-bound PAHs were discussed, the detail theoretical discussion information can be found in Text S1 in the supporting information. We illustrate that decrease of ambient temperature would result in the increase of individual PAH in the particulate phase assuming a constant total concentration in the air. The decrease of SR can indeed lower concentrations of hydroxyl radical [OH] and accumulate PAHs in the air, resulting in the increase of PAHs concentrations. And low height of boundary layer can inhibit the vertical diffusion of PAHs, which leads to PAHs accumulation and increased concentrations. As Figure 4 showed, PAHs exhibited strong negative correlations with temperature (T), solar radiation (SR) and the boundary layer height (~~BHL~~BLH), especially in the northern China. This indicated that the unfavorable meteorological conditions, such as low levels of temperature, solar radiation and ~~BHL~~ BLH could lead to PAHs accumulation in the air (Sofuoglu et al., 2001; Callén et al., 2014; Lin et al., 2015a; Li et al., 2016a). In fact, annual averages of T, SR and ~~BHL~~ BLH in the northern China were all significant lower than those in the southern China ($p<0.05$, Table S4), which could indeed cause the accumulation of PAHs in the air of the northern China. In addition, low temperature in the northern China would promote the condensation of semi-volatile PAHs on particles (Wang et al., 2011; Ma et al., 2020). At the

315 southern sites, the negative correlations between PAHs and meteorological parameters (SR and
316 ~~BHL~~BLH) were not as strong as those in the northern sites. This implied that the adverse
317 influence of meteorological conditions on PAHs pollution in the southern China might be less
318 significant than that in the northern China. Then we divide the one-year data into warm and
319 cold seasons based on the ambient temperature. As Figure S10 showed, at most sites in the
320 northern and southern China, PAHs negatively correlated with temperature (T), boundary layer
321 height (BLH) and solar radiation (SR) in both cold (T < 10 ° C) and warm (T > 10 ° C) seasons.
322 Thus, coupled with theoretical discussion, we suggested that worsened PAH pollution in winter
323 partly caused by adverse meteorological conditions.

324 For PAHs emission, there are apparent differences in sources and strength between the
325 northern and southern regions. For instance, there is central heating ~~a heating season~~ during
326 winter in the northern China, but not so in the southern China. The residential heating during
327 ~~winter~~ cold period in the northern China could consume large amounts of coal and biofuel, and
328 release substantial PAHs into the air (Liu et al., 2008; Xue et al., 2016). Consequently,
329 atmospheric levels of PAHs in the northern China were much higher than those in the southern
330 China. Since central heating systems start heat supply simultaneously within each region in the
331 northern China~~each northern region~~, atmospheric PAHs should increase synchronously within
332 the northern regions of China. To check the spatial homogeneity of PAHs on a regional scale,
333 we analyzed the correlation of PAHs between paired sites within each region. As Table 2
334 exhibited, PAHs varied synchronously and correlated well at the paired sites in the northern
335 China ($p<0.001$). And closer distance between sites, stronger correlations were observed. The
336 spatial synchronized trends~~homogeneity~~ of PAHs observed in the northern regions of China

probably resulted from the synchronous variation of PAHs emission in the northern China. In the southern China, although the distances between paired sites were closer than those in the northern regions, the correlations between sites within a region was weaker. This indicated that there might be more local emission which sources and strength vary place to place in the southern China.

We applied diagnostic ratios of PAH isomers to identify major sources of atmospheric PAHs. The ratios of IcdP/(IcdP+BghiP) and Flu/(Flu+Pyr) have been widely used to distinguish possible sources of PAHs (Aceves and Grimalt, 1993; Zhang et al., 2005; Ding et al., 2007; Gao et al., 2012; Lin et al., 2015a; Ma et al., 2018). As summarized by Yunker et al. (2002), the petroleum boundary ratios for IcdP/(IcdP+BghiP) and Flu/(Flu+Pyr) are close to 0.20 and 0.40, respectively; for petroleum combustion, the ratios of IcdP/(IcdP+BghiP) and Flu/(Flu+Pyr) range from 0.20 to 0.50 and 0.40 to 0.50, respectively; and the combustions of grass, wood and coal have the ratios higher than 0.50 for both IcdP/(IcdP+BghiP) and Flu/(Flu+Pyr). As Figure 5 showed, the ratios of Flu/(Flu+Pyr) at the 12 sites ranged from 0.49 to 0.76, suggesting that biomass (grass/wood) burning and coal combustion were the major sources. And the ratios of IcdP/(IcdP+BghiP) were in the range of 0.32 to 0.62, indicating that besides biomass and coal combustion, petroleum combustion, especially vehicle exhaust was also an important source of atmospheric PAHs. Thus, as identified by the diagnostic ratios, biomass burning, coal combustion and petroleum combustion were major sources of atmospheric PAHs over China. This is also confirmed by the significant correlations of $\sum_{24}$ PAHs with the typical tracers of biomass burning (levoglucosan), coal combustion (picene) and vehicle exhaust (hopanes) ~~This is also confirmed by the significant correlations of $\sum_{24}$PAHs with the biomass burning tracer,~~

~~levoglucosan, the coal combustion tracer, picene, and the vehicle exhaust tracer, hopanes~~ at most sites (Figure 6). As global emission inventories showed, PAHs in the atmosphere were mainly released from the incomplete combustion processes including coal combustion, biomass burning and vehicle exhaust (Shen et al., 2013a).

To further attribute PAHs sources, we employed the PMF model to quantify source contributions to atmospheric PAHs at the 12 sites in China. Three factors were identified, and the factor profile resolved ~~and the typical factor profiles~~ by PMF were presented in Figure ~~S6~~S11. The first factor was identified as biomass burning, as it had high loadings of the biomass burning tracer, levoglucosan and light weight molecular PAHs such as Phe, Ant, Flu and Pyr which are largely emitted from biomass burning (Li et al., 2016b). The second factor was considered to be coal combustion, as it was characterized by high fractions of the coal combustion marker, picene and the high molecular weight PAHs ~~including DahA and BghiP~~ (~~Oros and Simoneit, 2000~~Shen et al., 2013b). The third factor was regarded as vehicle exhaust, as it was featured by presence of hopanes, which are molecular markers tracking vehicle exhaust ~~widely used as the tracers of traffic emission~~ (Cass, 1998; Dai et al., 2015). As Figure ~~S7~~ S12 showed, there was significant agreement between the predicted and measured PAHs at each site (R^2 in the range of 0.78 to 0.99, $p<0.001$). As the emission inventory of PAHs in China showed, residential/commercial, industrial and transportation were the major sectors of atmospheric PAHs in 2013 (Figure ~~S8~~S13, http://inventory.pku.edu.cn). Residential/commercial and industrial sectors mainly consumed coal and biofuel while transportation consumed oil (Shen et al., 2013a). Thus, the mainly sources of PAHs in China were coal combustion, biomass burning and petroleum combustion (especially vehicle exhaust).

Figure 7a presents atmospheric PAHs emitted from different sources in China. In the northern China, coal combustion was the ~~predominant~~ major source of atmospheric PAHs (73.6 ng m^{-3}, 84.2% of $\sum_{24}$PAHs), followed by biomass burning (11.8 ng m^{-3} and 13.5%) and vehicle exhaust (2.0 ng m^{-3} and 2.3%). In the southern China, coal combustion (9.6 ng m^{-3} and 54.8%) and biomass burning (6.8 ng m^{-3} and 39.0%) were the major contributors, followed by vehicle exhaust (1.1 ng m^{-3} and 6.2%). Atmospheric PAHs emitted from the three sources in the northern China were all higher than those in the southern China, especially from coal combustion. Thus, coal combustion was the most important source of atmospheric PAHs in China and caused large increases in PAHs pollution in the northern China. As China statistics yearbook recorded (http://www.stats.gov.cn/english/Statisticaldata/AnnualData/), coal was the dominant fuel in China, accounting for ~~65.2%~~70.6% (~~20~~24.1 ×10^8 tons of Standard Coal Equivalent, SCE) of total primary energy consumption in ~~2007~~2012, followed by crude oil ~~17.2~~19.9% (~~5.3~~6.7 ×10^8 tons of SCE) ~~and biofuel 8.3% (2.5 ×10^8 tons of SCE)~~ and other types of energy 9.5%, including biofuel, natural gas, hydro power, nuclear power and other power (3.2 ×10^8 tons of SCE). Although the biofuel consumption was lower than crude oil, the poor combustion conditions during residential biofuel burning could led to higher PAHs emissions as compared to petroleum combustion.

We further compared our results with those in the PAHs emission inventory of China (http://inventory.pku.edu.cn) (Figure ~~S9~~S14). Our source apportionment results focused on fuel types, while the emission inventory classified the sources into 6 socioeconomic sectors (residential & commercial activities, industry, energy production, agriculture, deforestation & wildfire, and transportation). Since the transportation mainly used liquid petroleum (gasoline

and diesel) and the rest sectors mainly consumed solid fuels (coal and biomass), we grouped these sectors into liquid petroleum combustion and solid fuel burning to directly compare with our results. As Figure ~~S9~~ S14 showed, both our observation and emissions inventory demonstrated that the PAHs contributions from solid fuel burning was higher in the northern China, while the PAHs contributions from liquid petroleum combustion was higher in the southern China.

Atmospheric PAHs emitted from different sources at urban, sub-urban and remote sites (Figure 7b) and different size particles (Figure 7c) were discussed. At urban and sub-urban sites, coal combustion was the largest source of $\sum_{24}$PAHs (70.4 ng m^{-3}, 85.1% and 30.5 ng m^{-3}, 63.5%), followed by biomass burning (10.1 ng m^{-3}, 12.2% and 16.3 ng m^{-3}, 33.9%) and vehicle emission (2.2 ng m^{-3}, 2.6% and 1.2 ng m^{-3}, 2.5%), while at remote sites the contributions of coal combustion (9.1 ng m^{-3}, 50.6%) and biomass burning (7.8 ng m^{-3}, 43.7%) were comparable and vehicle emission (1.0 ng m^{-3}, 5.7%) had minor contributions. The major sources of $\sum_{24}$PAHs varied among different size particles in the northern and southern China (Figure 7c). For $PM_{>3.3}$-bound PAHs, the contributions of coal combustion (50.3%) and biomass burning (48.4%) were comparable in the northern China, while biomass burning (71.0%) was the largest source in the southern China. For $PM_{1.1\text{-}3.3}$-bound PAHs, coal combustion (66.7%) was the dominated source in the northern China, whereas the percentage of biomass burning (53.7%) was larger than that of coal combustion (40.4%) in the southern China. For $PM_{1.1}$-bound PAHs, coal combustion was the dominated source in the northern (66.6%) and southern (59.3%) China.

Source apportionment of BaP_{eq} in different regions (Figure 7d), sampling sites (Figure 7e) and size particles (Figure 7f) were also discussed. Unlike $\sum_{24}$PAHs, coal combustion was the

predominant source of BaP_{eq} in the northern (8.1 ng m^{-3} and 95.7%) and the southern (1.1 ng m^{-3} and 84.7%) China. The contributions of coal contribution at urban sites (8.3 ng m^{-3} and 96.4%) were larger than those at sub-urban (3.3 ng m^{-3} and 90.8%) and remote (1.0 ng m^{-3} and 82.5%) sites. Coal combustion was the dominate source in different size particles. And its contributions to $PM_{>3.3}$, $PM_{1.1\text{-}3.3}$ and $PM_{1.1}$-bound PAHs in the northern China (87.3%, 95.6% and 96.9%) were all larger than those in the southern China (76.8%, 87.3% and 88.2%).

Here, we concluded that the unfavorable meteorological conditions and intensive emission especially in coal combustion together led to severe PAHs pollution and high cancer risk in the atmosphere of the northern China.

3.4 Nationwide increase of PAHs pollution and health risk during winter

Figure 8 exhibits monthly variations of BaP_{eq} and ILCR at the 12 sites. BaP_{eq} levels were the highest in winter and the lowest in summer at all sites. As Figure 8 showed, the enhancement of BaP_{eq} from summer to winter ranged from 1.05 (SY) to 32.5 (SPT). And such an enhancement was much more significant at the northern sites than the southern sites. Hence, ILCR was significantly enhanced in winter, especially in the northern China (Figure 8) and was much higher than the acceptable risk level of 1.0×10^{-6} in US (USEPA, 1991). Previous studies in different cities of China also reported such a winter-high trend of atmospheric PAHs (Liu et al., 2017b; Ma et al., 2018; Shen et al., 2019). Thus, there is a nationwide increase of PAHs pollution during winter in China.

The winter-high feature of PAHs pollution should result from the impacts of meteorological conditions and source emissions. The winter to summer ratios of PAHs correlated well with that for temperature (Figure ~~S10~~S15). And T, SR and ~~BHL~~ BLH were all

447 the lowest during winter and the highest during summer (Table S5-7). Coupled with the
448 negative correlations between PAHs and meteorological factors (Figure 4), the unfavorable
449 meteorological conditions in wintertime did account for the increase in PAHs pollution.

450 Moreover, PAHs emitted from coal combustion and biomass burning apparently elevated
451 during fall-winter (Figure 9). In the northern China, central heating systems in urban areas
452 usually start from November to next March. Meanwhile residential heating in the rural areas of
453 northern China consumes substantial coal and biofuel (Xue et al., 2016). Thus, the energy
454 consumption in the residential sector is dramatically enhanced during fall-winter (Xue et al.,
455 2016). In the southern China, although there is no central heating system in urban areas, power
456 plant and industry consume large amounts of coal. And there is also residential coal/biofuel
457 consumption for heating during winter as well as cooking in rural areas (Zhang et al., 2013; Xu
458 et al., 2015). In addition, open burning of agriculture residuals which accounts for a major
459 fraction of the total biomass burning in China will significantly increase during fall-winter
460 harvest seasons in the southern China (Zhang et al., 2013). Our observation and emissions
461 inventory witnessed similar monthly trends that the PAHs from solid fuel combustion (coal and
462 biomass) apparently elevated during fall-winter in the northern and southern China (Figure
463 ~~S11~~S16). Previous field studies also found that the contributions of coal combustion and
464 biomass burning to PAHs elevated during fall-winter (Lin et al., 2015a; Yu et al., 2016). Thus,
465 we concluded that the unfavorable meteorological conditions and intensive source emission
466 together led to the increase of PAHs pollution during winter.

467 **Data availability**

468 The data are given in the Supplement.

Author contributions

Qingqing Yu analyzed the data, wrote the paper and performed data interpretation. Quanfu He and Ruqin Shen analyzed the samples. Weiqiang Yang ran the PMF model and helped with the interpretation. Ming Zhu, Sheng Li and Runqi Zhang provided the meteorological data and prepared the related interpretation. Yanli Zhang and Xinhui Bi gave many suggestions about the results and discussion. Yuesi Wang helped the field observation and performed data interpretation. Xiang Ding, Ping'an Peng and Xinming Wang performed data interpretation, reviewed and edited this paper.

Competing interests

The authors declare that they have no conflict of interest.

Acknowledgement

This study was funded by the National Natural Science Foundation of China (41530641/4191101024/41722305/41907196), the National Key Research and Development Program (2016YFC0202204/2018YFC0213902), the Chinese Academy of Sciences (XDA05100104/QYZDJ-SSW-DQC032), and Guangdong Foundation for Science and Technology Research (2019B121205006/2017BT01Z134/ 2020B1212060053).

References

Aceves, M., Grimalt, J.O., 1993. Seasonally dependent size distributions of aliphatic and polycyclic aromatic hydrocarbons in urban aerosols from densely populated areas. Environ. Sci. Technol. 27, 2896-2908.

Armstrong, B., Hutchinson, E., Unwin, J., Fletcher, T., 2004. Lung cancer risk after exposure to polycyclic aromatic hydrocarbons: A review and meta-analysis. Environ. Health. Persp. 112, 970-978.

Belis, C.A., Cancelinha, J., Duane, M., Forcina, V., Pedroni, V., Passarella, R., Tanet, G., Douglas, K., Piazzalunga, A., Bolzacchini, E., Sangiorgi, G., Perrone, M.G., Ferrero, L., Fermo, P., Larsen, B.R., 2011. Sources for PM air pollution in the Po Plain, Italy: I. Critical comparison of methods for estimating biomass burning contributions to benzo(a)pyrene. Atmos. Environ. 45, 7266-7275.

Bi, X.H., Sheng, G.Y., Peng, P.A., Chen, Y.J., Zhang, Z.Q., Fu, J.M., 2003. Distribution of particulate- and vapor-phase n-alkanes and polycyclic aromatic hydrocarbons in urban atmosphere of Guangzhou, China. Atmos. Environ. 37, 289-298.

Brown, A.S., Brown, R.J.C., Coleman, P.J., Conolly, C., Sweetman, A.J., Jones, K.C., Butterfield, D.M., Sarantaridis, D., Donovan, B.J., Roberts, I., 2013. Twenty years of measurement of polycyclic aromatic hydrocarbons (PAHs) in UK ambient air by nationwide air quality networks. Environ. Sci.-Proc. Imp. 15, 1199-1215.

Callén, M.S., Iturmendi, A., López, J.M., 2014. Source apportionment of atmospheric $PM_{2.5}$-bound polycyclic aromatic hydrocarbons by a PMF receptor model. Assessment of potential risk for human health. Environ. Pollut. 195, 167-177.

508 Cass, G.R., 1998. Organic molecular tracers for particulate air pollution sources. Trac.-Trend
509 Anal. Chem. 17, 356-366.
510 Chung, Y., Dominici, F., Wang, Y., Coull, B.A., Bell, M.L., 2015. Associations between long-
511 term exposure to chemical constituents of fine particulate matter ($PM_{2.5}$) and mortality in
512 medicare enrollees in the eastern United States. Environ. Health Persp. 123, 467-474.
513 Cohen, A.J., Brauer, M., Burnett, R., Anderson, H.R., Frostad, J., Estep, K., Balakrishnan, K.,
514 Brunekreef, B., Dandona, L., Dandona, R., Feigin, V., Freedman, G., Hubbell, B., Jobling,
515 A., Kan, H., Knibbs, L., Liu, Y., Martin, R., Morawska, L., Pope, C.A., Shin, H., Straif,
516 K., Shaddick, G., Thomas, M., van Dingenen, R., van Donkelaar, A., Vos, T., Murray,
517 C.J.L., Forouzanfar, M.H., 2017. Estimates and 25-year trends of the global burden of
518 disease attributable to ambient air pollution: An analysis of data from the Global Burden
519 of Diseases Study 2015. Lancet 389, 1907-1918.
520 Dai, S., Bi, X., Chan, L.Y., He, J., Wang, B., Wang, X., Peng, P., Sheng, G., Fu, J., 2015.
521 Chemical and stable carbon isotopic composition of $PM_{2.5}$ from on-road vehicle emissions
522 in the PRD region and implications for vehicle emission control policy. Atmos. Chem.
523 Phys. 15, 3097-3108.
524 Ding, X., He, Q.F., Shen, R.Q., Yu, Q.Q., Wang, X.M., 2014. Spatial distributions of secondary
525 organic aerosols from isoprene, monoterpenes, beta-caryophyllene, and aromatics over
526 China during summer. J. Geophys. Res.-Atmos. 119, 11877-11891.
527 Ding, X., Wang, X.M., Xie, Z.Q., Xiang, C.H., Mai, B.X., Sun, L.G., Zheng, M., Sheng, G.Y.,
528 Fu, J.M., Poschl, U., 2007. Atmospheric polycyclic aromatic hydrocarbons observed over
529 the North Pacific Ocean and the Arctic area: Spatial distribution and source identification.

Atmos. Environ. 41, 2061-2072.

Dong, W., Pan, L., Li, H., Miller, M.R., Loh, M., Wu, S., Xu, J., Yang, X., Shan, J., Chen, Y., Deng, F., Guo, X., 2018. Association of size-fractionated indoor particulate matter and black carbon with heart rate variability in healthy elderly women in Beijing. Indoor Air 28, 373-382.

Duan, J.C., Bi, X.H., Tan, J.H., Sheng, G.Y., Fu, J.M., 2007. Seasonal variation on size distribution and concentration of PAHs in Guangzhou city, China. Chemosphere 67, 614-622.

Gao, B., Guo, H., Wang, X.M., Zhao, X.Y., Ling, Z.H., Zhang, Z., Liu, T.Y., 2012. Polycyclic aromatic hydrocarbons in $PM_{2.5}$ in Guangzhou, southern China: Spatiotemporal patterns and emission sources. J. Hazard. Mater. 239, 78-87.

Gao, B., Guo, H., Wang, X.M., Zhao, X.Y., Ling, Z.H., Zhang, Z., Liu, T.Y., 2013. Tracer-based source apportionment of polycyclic aromatic hydrocarbons in $PM_{2.5}$ in Guangzhou, southern China, using positive matrix factorization (PMF). Environ. Sci. Pollut. R. 20, 2398-2409.

Gao, B., Wang, X.M., Zhao, X.Y., Ding, X., Fu, X.X., Zhang, Y.L., He, Q.F., Zhang, Z., Liu, T.Y., Huang, Z.Z., Chen, L.G., Peng, Y., Guo, H., 2015. Source apportionment of atmospheric PAHs and their toxicity using PMF: Impact of gas/particle partitioning. Atmos. Environ. 103, 114-120.

Gao, B., Yu, J.Z., Li, S.X., Ding, X., He, Q.F., Wang, X.M., 2011. Roadside and rooftop measurements of polycyclic aromatic hydrocarbons in $PM_{2.5}$ in urban Guangzhou: Evaluation of vehicular and regional combustion source contributions. Atmos. Environ.

552 45, 7184-7191.
553 Garrido, A., Jiménez-Guerrero, P., Ratola, N., 2014. Levels, trends and health concerns of
554 atmospheric PAHs in Europe. Atmos. Environ. 99, 474-484.
555 Gu, Z.P., Feng, J.L., Han, W.L., Li, L., Wu, M.H., Fu, J.M., Sheng, G.Y., 2010. Diurnal
556 variations of polycyclic aromatic hydrocarbons associated with $PM_{2.5}$ in Shanghai, China.
557 J. Environ. Sci. 22, 389-396.
558 Guo, H., Lee, S.C., Ho, K.F., Wang, X.M., Zou, S.C., 2003. Particle-associated polycyclic
559 aromatic hydrocarbons in urban air of Hong Kong. Atmos. Environ. 37, 5307-5317.
560 Hayakawa, K., Tang, N., Nagato, E.G., Toriba, A., Sakai, S., Kano, F., Goto, S., Endo, O.,
561 Arashidani, K.-i., Kakimoto, H., 2018. Long term trends in atmospheric concentrations of
562 polycyclic aromatic hydrocarbons and nitropolycyclic aromatic hydrocarbons: A study of
563 Japanese cities from 1997 to 2014. Environ. Pollut. 233, 474-482.
564 He, J.B., Fan, S.X., Meng, Q.Z., Sun, Y., Zhang, J., Zu, F., 2014. Polycyclic aromatic
565 hydrocarbons (PAHs) associated with fine particulate matters in Nanjing, China:
566 Distributions, sources and meteorological influences. Atmos. Environ. 89, 207-215.
567 Hong, W.J., Jia, H.L., Ma, W.L., Sinha, R.K., Moon, H.-B., Nakata, H., Minh, N.H., Chi, K.H.,
568 Li, W.L., Kannan, K., Sverko, E., Li, Y.F., 2016. Distribution, fate, inhalation exposure
569 and lung cancer risk of atmospheric polycyclic aromatic hydrocarbons in aome Asian
570 countries. Environ. Sci. Technol. 13, 7163-7174.
571 Huang, X.F., He, L.Y., Hu, M., Zhang, Y.H., 2006. Annual variation of particulate organic
572 compounds in $PM_{2.5}$ in the urban atmosphere of Beijing. Atmos. Environ. 40, 2449-2458.
573 Inomata, Y., Kajino, M., Sato, K., Ohara, T., Kurokawa, J. I., Ueda, H., Tang, N., Hayakawa,

574 K., Ohizumi, T., Akimoto, H., 2012. Emission and atmospheric transport of particulate
575 PAHs in Northeast Asia. Environ. Sci. Technol. 46, 4941-4949.
576 International Agency for Research on Cancer, 2001. Overall Evaluations of Carcinogenicity to
577 Humans.
578 Jaward, F.M., Farrar, N.J., Harner, T., Sweetman, A.J., Jones, K.C., 2004. Passive air sampling
579 of polycyclic aromatic hydrocarbons and polychlorinated naphthalenes across Europe.
580 Environ. Toxicol. Chem. 23, 1355-1364.
581 John, K., Ragavan, N., Pratt, M.M., Singh, P.B., Al-Buheissi, S., Matanhelia, S.S., Phillips,
582 D.H., Poirier, M.C., Martin, F.L., 2009. Quantification of phase I/II metabolizing enzyme
583 gene expression and polycyclic aromatic hydrocarbon–DNA adduct levels in human
584 prostate. The Prostate 69, 505-519.
585 Kim, K.H., Jahan, S.A., Kabir, E., Brown, R.J.C., 2013. A review of airborne polycyclic
586 aromatic hydrocarbons (PAHs) and their human health effects. Environ. Int. 60, 71-80.
587 Kuo, C.Y., Hsu, Y.W., Lee, H.S., 2003. Study of human exposure to particulate PAHs using
588 personal air samplers. Arch. Environ. Con. Tox. 44, 0454-0459.
589 Lang, C., Tao, S., Wang, X.J., Zhang, G., Li, J., Fu, J.M., 2007. Seasonal variation of polycyclic
590 aromatic hydrocarbons (PAHs) in Pearl River Delta region, China. Atmos. Environ. 41,
591 8370-8379.
592 Larsen, R.K., Baker, J.E., 2003. Source apportionment of polycyclic aromatic hydrocarbons in
593 the urban atmosphere: A comparison of three methods. Environ. Sci. Technol. 37, 1873-
594 1881.
595 Li, H.Y., Guo, L.L., Cao, R.F., Gao, B., Yan, Y.L., He, Q.S., 2016a. A wintertime study of $PM_{2.5}$-

596 bound polycyclic aromatic hydrocarbons in Taiyuan during 2009-2013: Assessment of
597 pollution control strategy in a typical basin region. Atmos. Environ. 140, 404-414.
598 Li, H., Li, H., Zhang, L., Cheng, M., Guo, L., He, Q., Wang, X., Wang, Y., 2019. High cancer
599 risk from inhalation exposure to PAHs in Fenhe Plain in winter: A particulate size
600 distribution-based study. Atmos. Environ. 216, 116924.
601 Li, J., Zhang, G., Li, X.D., Qi, S.H., Liu, G.Q., Peng, X.Z., 2006. Source seasonality of
602 polycyclic aromatic hydrocarbons (PAHs) in a subtropical city, Guangzhou, South China.
603 Sci. Total Environ. 355, 145-155.
604 Li, X., Yang, Y., Xu, X., Xu, C., Hong, J., 2016b. Air pollution from polycyclic aromatic
605 hydrocarbons generated by human activities and their health effects in China. J. Clean
606 Prod. 112, 1360-1367.
607 Lin, Y., Ma, Y.Q., Qiu, X.H., Li, R., Fang, Y.H., Wang, J.X., Zhu, Y.F., Hu, D., 2015a. Sources,
608 transformation, and health implications of PAHs and their nitrated, hydroxylated, and
609 oxygenated derivatives in $PM_{2.5}$ in Beijing. J. Geophys. Res.- Atmos. 120, 7219-7228.
610 Lin, Y., Qiu, X.H., Ma, Y.Q., Ma, J., Zheng, M., Shao, M., 2015b. Concentrations and spatial
611 distribution of polycyclic aromatic hydrocarbons (PAHs) and nitrated PAHs (NPAHs) in
612 the atmosphere of North China, and the transformation from PAHs to NPAHs. Environ.
613 Pollut. 196, 164-170.
614 Liu, B., Xue, Z., Zhu, X., Jia, C., 2017a. Long-term trends (1990–2014), health risks, and
615 sources of atmospheric polycyclic aromatic hydrocarbons (PAHs) in the U.S. Environ.
616 Pollut. 220, 1171-1179.
617 Liu, D., Lin, T., Syed, J.H., Cheng, Z.N., Xu, Y., Li, K.C., Zhang, G., Li, J., 2017b.

Concentration, source identification, and exposure risk assessment of $PM_{2.5}$-bound parent PAHs and nitro-PAHs in atmosphere from typical Chinese cities. Sci. Rep.-UK. 7, 10398.

Liu, S.Z., Tao, S., Liu, W.X., Dou, H., Liu, Y.N., Zhao, J.Y., Little, M.G., Tian, Z.F., Wang, J.F., Wang, L.G., Gao, Y., 2008. Seasonal and spatial occurrence and distribution of atmospheric polycyclic aromatic hydrocarbons (PAHs) in rural and urban areas of the North Chinese Plain. Environ. Pollut. 156, 651-656.

Liu, S.Z., Tao, S., Liu, W.X., Liu, Y.N., Dou, H., Zhao, J.Y., Wang, L.G., Wang, J.F., Tian, Z.F., Gao, Y., 2007a. Atmospheric polycyclic aromatic hydrocarbons in north China: A winter-time study. Environ. Sci. Technol. 41, 8256-8261.

Liu, X., Zhang, G., Li, J., Cheng, H.R., Qi, S.H., Li, X.D., Jones, K.C., 2007b. Polycyclic aromatic hydrocarbons (PAHs) in the air of Chinese cities. J. Environ. Monitor. 9, 1092-1098.

Liu, Y.J., Zhu, L.Z., Shen, X.Y., 2001. Polycyclic aromatic hydrocarbons (PAHs) in indoor and outdoor air of Hangzhou, China. Environ. Sci. Technol. 35, 840-844.

Lv, Y., Li, X., Xu, T.T., Cheng, T.T., Yang, X., Chen, J.M., Iinuma, Y., Herrmann, H., 2016. Size distributions of polycyclic aromatic hydrocarbons in urban atmosphere: Sorption mechanism and source contributions to respiratory deposition. Atmos. Chem. Phys. 16, 2971-2983.

Ma, W.L., Liu, L.Y., Jia, H.L., Yang, M., Li, Y.F., 2018. PAHs in Chinese atmosphere Part I: Concentration, source and temperature dependence. Atmos. Environ. 173, 330-337.

Ma, W.L., Zhu, F.J., Hu, P.T., Qiao, L.N., Li, Y.F., 2020. Gas/particle partitioning of PAHs based on equilibrium-state model and steady-state model. Sci. Total Environ. 706. 136029.

Mastral, A.M., Callén, M.S., 2000. A review on polycyclic aromatic hydrocarbon (PAH) emissions from energy generation. Environ. Sci. Technol. 34, 3051-3057.

Nisbet, I.C.T., Lagoy, P.K., 1992. Toxic equivalency factors (TEFs) for polycyclic aromatic hydrocarbons (PAHs). Regul. Toxicol. Pharm. 16, 290-300.

~~Oros, D.R., Simoneit, B.R.T., 2000. Identification and emission rates of molecular tracers in coal smoke particulate matter. Fuel 79, 515-536.~~

Polissar, A.V., Hopke, P.K., Paatero, P., 1998. Atmospheric aerosol over Alaska 2. Elemental composition and sources. J. Geophys. Res.- Atmos. 103, 19045-19057.

Shen, H.Z., Huang, Y., Wang, R., Zhu, D., Li, W., Shen, G.F., Wang, B., Zhang, Y.Y., Chen, Y.C., Lu, Y., Chen, H., Li, T.C., Sun, K., Li, B.G., Liu, W.X., Liu, J.F., Tao, S., 2013a. Global atmospheric emissions of polycyclic aromatic hydrocarbons from 1960 to 2008 and future predictions. Environ. Sci. Technol. 47, 6415-6424.

Shen, G.F., Tao, S., Chen, Y.C., Zhang, Y.Y., Wei, S.Y., Xue, M., Wang, B., Wang, R., Lu, Y., Li, W., Shen, H.Z., Huang, Y., Chen, H., 2013b. Emission characteristics for polycyclic aromatic hydrocarbons from solid fuels burned in domestic stoves in rural China. Environ. Sci. Technol. 47, 14485-14494.

Shen, R., Wang, Y., Gao, W., Cong, X., Cheng, L., Li, X., 2019. Size-segregated particulate matter bound polycyclic aromatic hydrocarbons (PAHs) over China: Size distribution, characteristics and health risk assessment. Sci. Total Environ. 685, 116-123.

Shrivastava, M., Lou, S., Zelenyuk, A., Easter, R.C., Corley, R.A., Thrall, B.D., Rasch, P.J., Fast, J.D., Massey Simonich, S.L., Shen, H., Tao, S., 2017. Global long-range transport and lung cancer risk from polycyclic aromatic hydrocarbons shielded by coatings of

662 organic aerosol. P. Natl. Acad. Sci. USA 114, 1246-1251.
663 Sofuoglu, A., Odabasi, M., Tasdemir, Y., Khalili, N.R., Holsen, T.M., 2001. Temperature
664 dependence of gas-phase polycyclic aromatic hydrocarbon and organochlorine pesticide
665 concentrations in Chicago air. Atmos. Environ. 35, 6503-6510.
666 Song, C.B., He, J.J., Wu, L., Jin, T.S., Chen, X., Li, R.P., Ren, P.P., Zhang, L., Mao, H.J., 2017.
667 Health burden attributable to ambient $PM_{2.5}$ in China. Environ. Pollut. 223, 575-586.
668 Sun, P., Blanchard, P., Brice, K.A., Hites, R.A., 2006. Trends in polycyclic aromatic
669 hydrocarbon concentrations in the Great Lakes atmosphere. Environ. Sci. Technol. 40,
670 6221-6227.
671 Tan, J.H., Bi, X.H., Duan, J.C., Rahn, K.A., Sheng, G.Y., Fu, J.M., 2006. Seasonal variation of
672 particulate polycyclic aromatic hydrocarbons associated with PM_{10} in Guangzhou, China.
673 Atmos. Res. 80, 250-262.
674 Tang, N., Suzuki, G., Morisaki, H., Tokuda, T., Yang, X.Y., Zhao, L.X., Lin, J.M., Kameda, T.,
675 Toriba, A., Hayakawa, K., 2017. Atmospheric behaviors of particulate-bound polycyclic
676 aromatic hydrocarbons and nitropolycyclic aromatic hydrocarbons in Beijing, China from
677 2004 to 2010. Atmos. Environ. 152, 354-361.
678 USEPA, 1991. Role of the baseline risk assessment in Superfund remedy-selection decisions.
679 Office of Solid Waste and Emergency Response, Washington.
680 Wang, G., Kawamura, K., Lee, S., Ho, K., Cao, J., 2006. Molecular, seasonal, and spatial
681 distributions of organic aerosols from fourteen Chinese cities. Environ. Sci. Technol. 40,
682 4619-4625.
683 Wang, G., Kawamura, K., Xie, M., Hu, S., Gao, S., Cao, J., An, Z., Wang, Z., 2009. Size-

684 distributions of n-alkanes, PAHs and hopanes and their sources in the urban, mountain and
685 marine atmospheres over East Asia. Atmos. Chem. Phys. 9, 8869-8882.
686 Wang, Q.Y., Kobayashi, K., Lu, S.L., Nakajima, D., Wang, W.Q., Zhang, W.C., Sekiguchi, K.,
687 Terasaki, M., 2016. Studies on size distribution and health risk of 37 species of polycyclic
688 aromatic hydrocarbons associated with fine particulate matter collected in the atmosphere
689 of a suburban area of Shanghai city, China. Environ. Pollut. 214, 149-160.
690 Wang, W.T., Simonich, S.L.M., Wang, W., Giri, B., Zhao, J.Y., Xue, M., Cao, J., Lu, X.X., Tao,
691 S., 2011. Atmospheric polycyclic aromatic hydrocarbon concentrations and gas/particle
692 partitioning at background, rural village and urban sites in the North China Plain. Atmos.
693 Res. 99, 197-206.
694 World Health Organization (WHO), 2000. Air Quality Guidelines for Europe, 2nd Edition,
695 World Health Organization Regional Office for Europe, Copenhagen.
696 Xu, H.J., Wang, X.M., Poesch, U., Feng, S.L., Wu, D., Yang, L., Li, S.X., Song, W., Sheng,
697 G.Y., Fu, J.M., 2008. Genotoxicity of total and fractionated extractable organic matter in
698 fine air particulate matter from urban Guangzhou: Comparison between haze and nonhaze
699 episodes. Environ. Toxicol. Chem. 27, 206-212.
700 Xu, J., Chang, S.Y., Yuan, Z.H., Jiang, Y., Liu, S.N., Li, W.Z., Ma, L.L., 2015. Regionalized
701 techno-economic assessment and policy analysis for biomass molded fuel in China.
702 Energies 8, 13846-13863.
703 Xu, S.S., Liu, W.X., Tao, S., 2006. Emission of polycyclic aromatic hydrocarbons in China.
704 Environ. Sci. Technol. 40, 702-708.
705 Xue, Y.F., Zhou, Z., Nie, T., Wang, K., Nie, L., Pan, T., Wu, X.Q., Tian, H.Z., Zhong, L.H., Li,

706 J., Liu, H.J., Liu, S.H., Shao, P.Y., 2016. Trends of multiple air pollutants emissions from
707 residential coal combustion in Beijing and its implication on improving air quality for
708 control measures. Atmos. Environ. 142, 303-312.
709 Yang, G.H., Wang, Y., Zeng, Y.X., Gao, G.F., Liang, X.F., Zhou, M.G., Wan, X., Yu, S.C., Jiang,
710 Y.H., Naghavi, M., Vos, T., Wang, H.D., Lopez, A.D., Murray, C.J.L., 2013. Rapid health
711 transition in China, 1990-2010: Findings from the Global Burden of Disease Study 2010.
712 Lancet 381, 1987-2015.
713 Yang, Y.Y., Guo, P.R., Zhang, Q., Li, D.L., Zhao, L., Mu, D.H., 2010. Seasonal variation,
714 sources and gas/particle partitioning of polycyclic aromatic hydrocarbons in Guangzhou,
715 China. Sci. Total Environ. 408, 2492-2500.
716 Yin, P., Guo, J., Wang, L., Fan, W., Lu, F., Guo, M., Moreno, S.B.R., Wang, Y., Wang, H., Zhou,
717 M., Dong, Z., 2020. Higher risk of cardiovascular disease associated with smaller size-
718 fractioned particulate matter. Environ. Sci. Technol. Let. 7, 95-101.
719 Yu, Q.Q., Gao, B., Li, G.H., Zhang, Y.L., He, Q.F., Deng, W., Huang, Z.H., Ding, X., Hu, Q.H.,
720 Huang, Z.Z., Wang, Y.J., Bi, X.H., Wang, X.M., 2016. Attributing risk burden of $PM_{2.5}$-
721 bound polycyclic aromatic hydrocarbons to major emission sources: Case study in
722 Guangzhou, south China. Atmos. Environ. 142, 313-323.
723 Yu, Q.Q., Yang, W.Q., Zhu, M., Gao, B., Li, S., Li, G.H., Fang, H., Zhou, H.S., Zhang, H.N.,
724 Wu, Z.F., Song, W., Tan, J.H., Zhang, Y.L., Bi, X.H., Chen, L.G., Wang, X.M., 2018.
725 Ambient $PM_{2.5}$-bound polycyclic aromatic hydrocarbons (PAHs) in rural Beijing:
726 Unabated with enhanced temporary emission control during the 2014 APEC summit and
727 largely aggravated after the start of wintertime heating. Environ. Pollut. 238, 532-542.

728 Yu, Y.X., Li, Q., Wang, H., Wang, B., Wang, X.L., Ren, A.G., Tao, S., 2015. Risk of human
729 exposure to polycyclic aromatic hydrocarbons: A case study in Beijing, China. Environ.
730 Pollut. 205, 70-77.
731 Yunker, M.B., Macdonald, R.W., Vingarzan, R., Mitchell, R.H., Goyette, D., Sylvestre, S., 2002.
732 PAHs in the Fraser River basin: A critical appraisal of PAH ratios as indicators of PAH
733 source and composition. Org. Geochem. 33, 489-515.
734 Zelenyuk, A., Imre, D., Beranek, J., Abramson, E., Wilson, J., Shrivastava, M., 2012. Synergy
735 between secondary organic aerosols and long-range transport of polycyclic aromatic
736 hydrocarbons. Environ. Sci. Technol. 46, 12459-12466.
737 Zhang, K., Zhang, B.Z., Li, S.M., Wong, C.S., Zeng, E.Y., 2012. Calculated respiratory
738 exposure to indoor size-fractioned polycyclic aromatic hydrocarbons in an urban
739 environment. Sci. Total Environ. 431, 245-251.
740 Zhang, Y.S., Shao, M., Lin, Y., Luan, S.J., Mao, N., Chen, W.T., Wang, M., 2013. Emission
741 inventory of carbonaceous pollutants from biomass burning in the Pearl River Delta
742 Region, China. Atmos. Environ. 76, 189-199.
743 Zhang, X.L., Tao, S., Liu, W.X., Yang, Y., Zuo, Q., Liu, S.Z., 2005. Source diagnostics of
744 polycyclic aromatic hydrocarbons based on species ratios: A multimedia approach.
745 Environ. Sci. Technol. 39, 9109-9114.
746 Zhang, Y.X., Tao, S., 2008. Seasonal variation of polycyclic aromatic hydrocarbons (PAHs)
747 emissions in China. Environ. Pollut. 156, 657-663.
748 Zhang, Y.X., Tao, S., 2009. Global atmospheric emission inventory of polycyclic aromatic
749 hydrocarbons (PAHs) for 2004. Atmos. Environ. 43, 812-819.

750 Zhang, Y.X., Tao, S., Cao, J., Coveney, R.M., 2007. Emission of polycyclic aromatic
751 hydrocarbons in China by county. Environ. Sci. Technol. 41, 683-687.
752 Zhang, Y., Shen, H., Tao, S., Ma, J., 2011. Modeling the atmospheric transport and outflow of
753 polycyclic aromatic hydrocarbons emitted from China. Atmos. Environ. 45, 2820-2827.
754 Zhang, Y.X., Tao, S., Shen, H.Z., Ma, J.M., 2009. Inhalation exposure to ambient polycyclic
755 aromatic hydrocarbons and lung cancer risk of Chinese population. P. Natl. Acad. Sci.
756 USA 106, 21063-21067.
757 Zhu, L.Z., Lu, H., Chen, S.G., Amagai, T., 2009. Pollution level, phase distribution and source
758 analysis of polycyclic aromatic hydrocarbons in residential air in Hangzhou, China. J.
759 Hazard. Mater. 162, 1165-1170.
760 Zhu, Y., Tao, S., Price, O.R., Shen, H.Z., Jones, K.C., Sweetman, A.J., 2015. Environmental
761 distributions of benzo[a]pyrene in China: Current and future emission reduction scenarios
762 explored using a spatially explicit multimedia fate model. Environ. Sci. Technol. 49,
763 13868-13877.
764

765 Table 1 PAHs concentration measured in this study and comparison with those of other large scale
766 observations.

Site/type	Sampling period	Sample type	# of sites	# of species	PAHs (ng/m^3)	Reference
China[a]	Oct, 2012-Sep, 2013	$PM_{1.1}$	12	24	3.4-126.2	This study
China[a]	Oct, 2012-Sep, 2013	$PM_{1.1-3.3}$	12	24	2.4-55.7	This study
China[a]	Oct, 2012-Sep, 2013	$PM_{>3.3}$	12	24	1.8-22.7	This study
China/Urban	2003	$PM_{2.5}$	14	18	1.7-701	Wang et al., 2006
China[b]	2005	PUF	40	20	374.5[e]	Liu et al., 2007
China/Urban	2013-2014	$PM_{2.5}$	9	16	14-210	Liu et al., 2017b
China/Urban	Aug, 2008-July, 2009	$PM_{2.5}$	11	16	75.4-478	Ma et al., 2018
China[c]	Jan, 2013-Dec, 2014	$PM_{9.0}$[e]	10	12	17.3-244.3	Shen et al., 2019
Great Lakes	1996-2003	PUF	7	16	0.59-70	Sun et al., 2006
Asian countries[d]	Sep, 2012-Aug, 2013	PUF	176	47	6.29-688	Hong et al., 2016
U.S.	1990-2014	PUF	169	15	52.6	Liu et al., 2017a
Japan	1997-2014	TSP	5	9	0.21-3.73	Hayakawa et al., 2018
Europe	2002	PUF	22	12	0.5-61.2	Jaward et al., 2004

767 a: including 5 urban sites, 3 sub-urban sites and 4 remote sites in China
768 b: including 37 cities and 3 rural locations in China
769 c: including 5 urban sites, 1 sub-urban site, 1 farmland site and 3 background sites in China
770 d: including 82 urban sites, 83 rural sites and 11 background sites in China, Japan, South Korea,
771 Vietnam, and India
772 e: the unit was ng/day
773

774 Table 2 Correlation coefficient (r), significance (p) of PAHs between paired sites in each region.

	Northern China			Southern China	
regions	north	northeast	northwest	east	southwest
paired sites	BJ-TY	HL-TYU	DH-SPT	WX-HF	KM-BN
distance between sites	400 km	450 km	940 km	280 km	380 km
r	0.97	0.80	0.63	0.77	-
p	<0.001	<0.001	0.001	<0.001	0.09

775

776

777

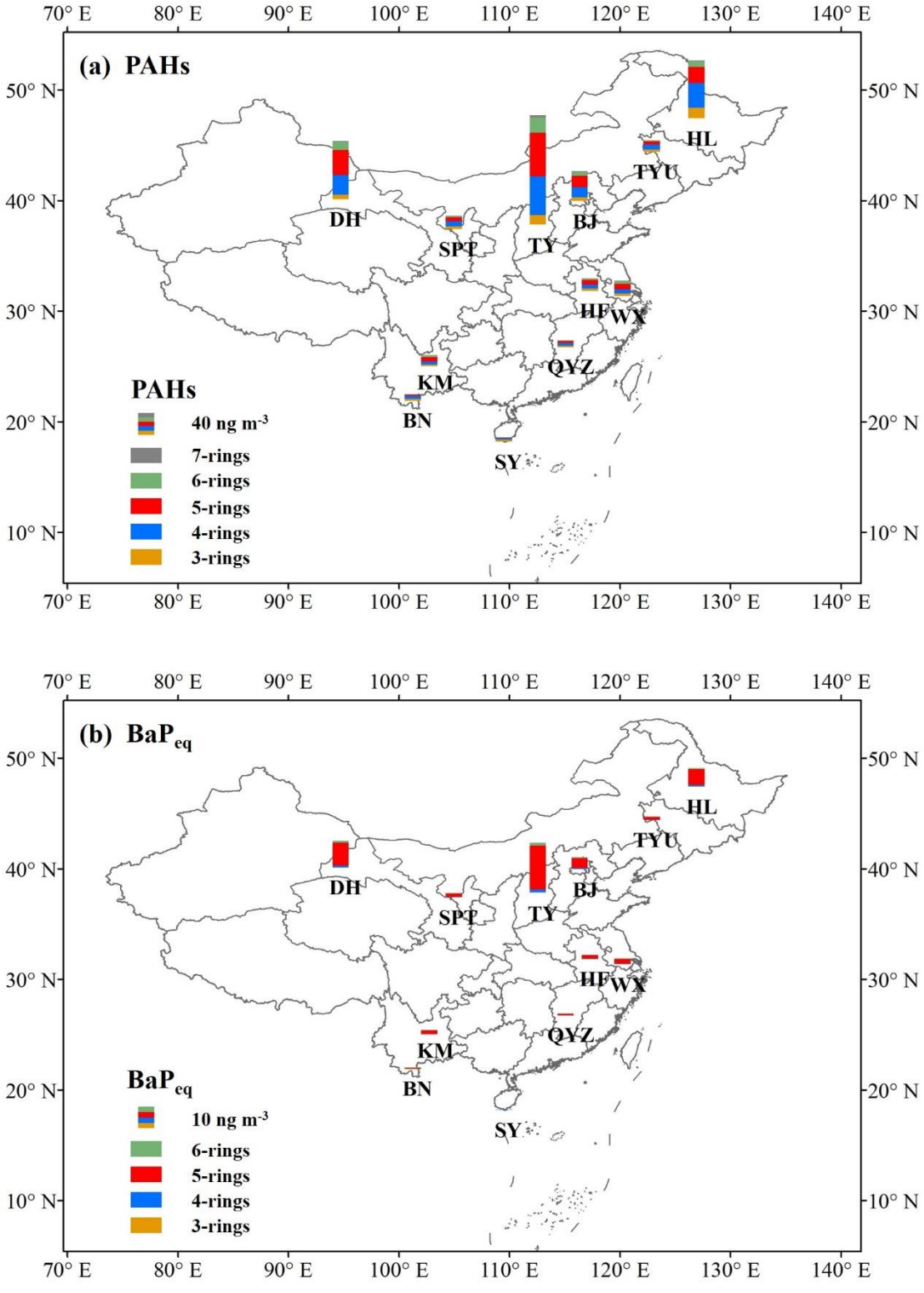

778

779 Figure 1 Annual averages of $\sum_{24}$PAHs (a) and BaP_{eq} (b) at 12 sites in China.

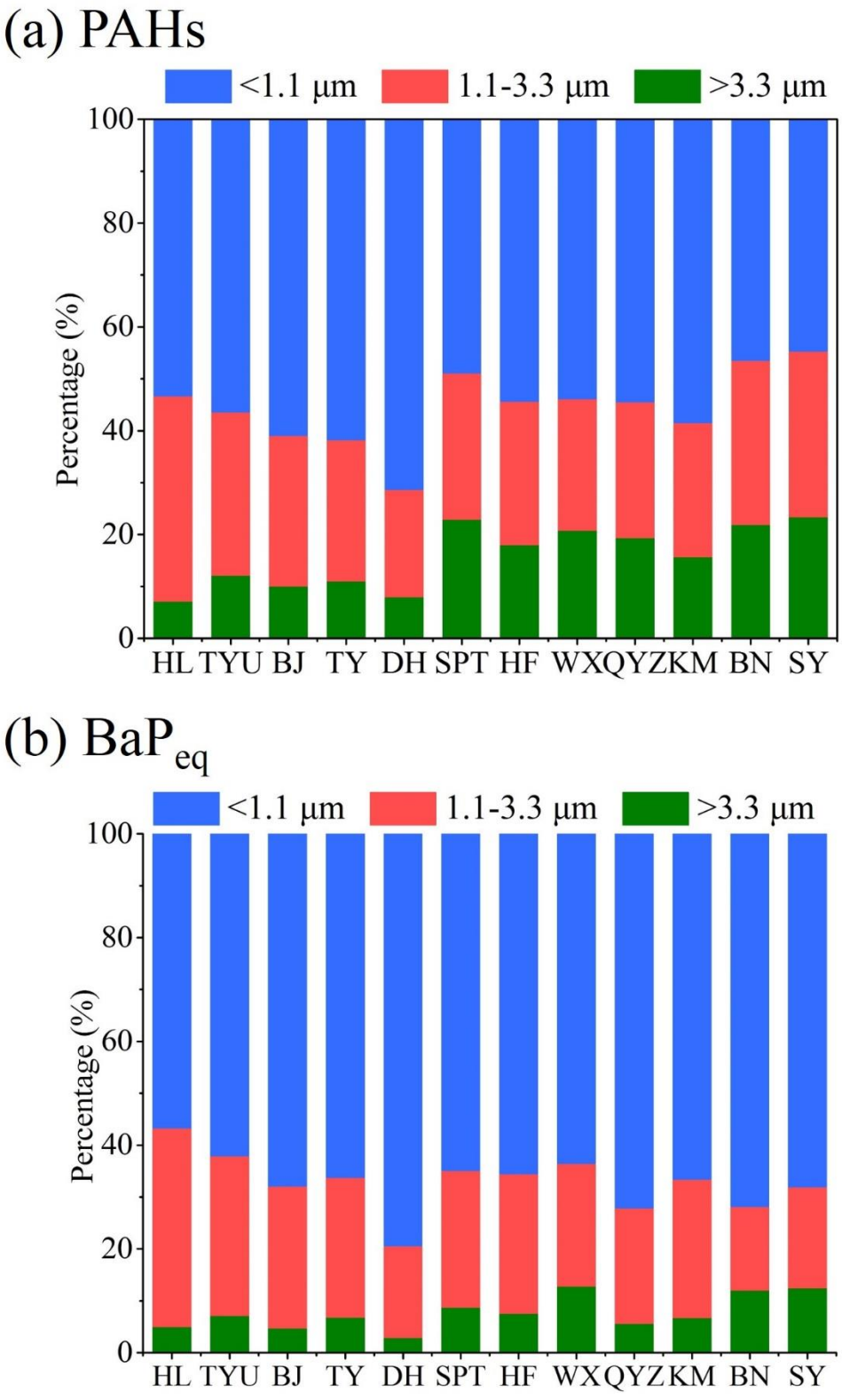

780

781 Figure 2 Size distribution of total measured PAHs (a) and BaP_{eq} (b) at 12 sites over China.

782

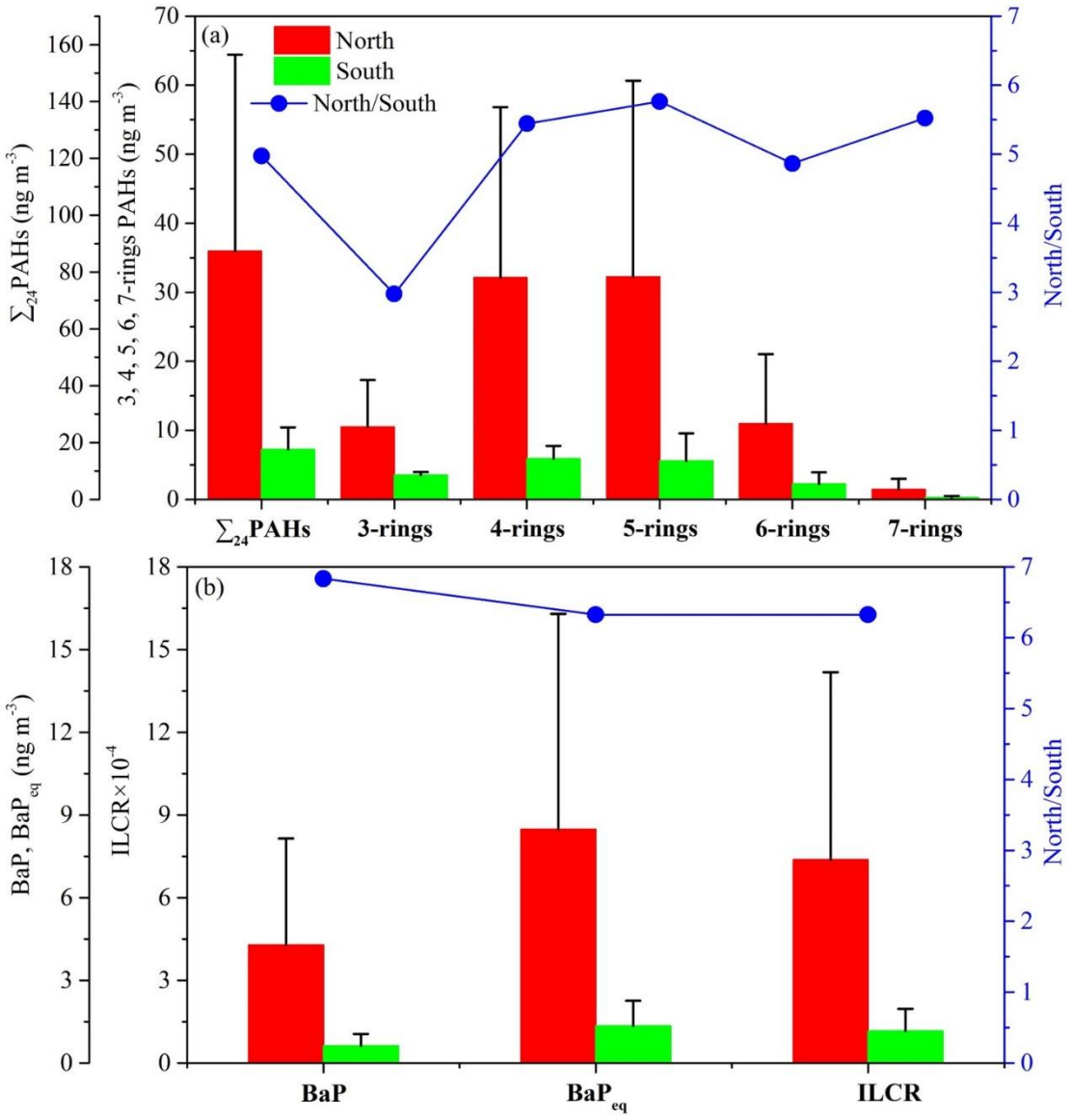

783

784 Figure 3 Comparison between the northern and the southern China in $\sum_{24}$PAHs, 3-7 rings PAHs

785 (a) and BaP, BaP$_{eq}$ and ILCR (b).

786

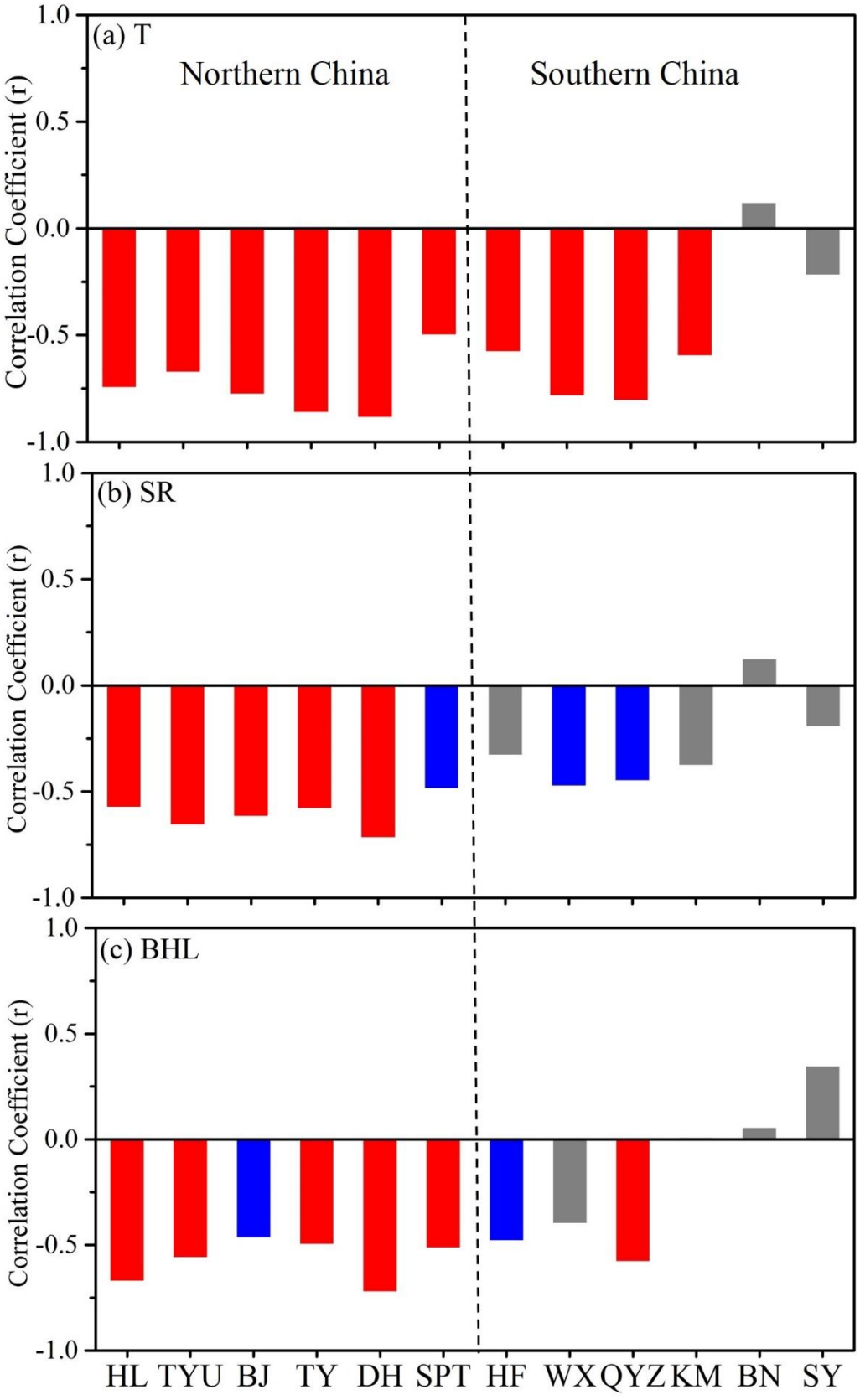

787

788 Figure 4 Correlation coefficient (r) of PAHs with T (a), SR (b) and ~~BHL~~ BLH (c) at 12 sites.

789 The red, blue and gray bars indicate $p<0.01$, $p<0.05$ and $p>0.05$, respectively.

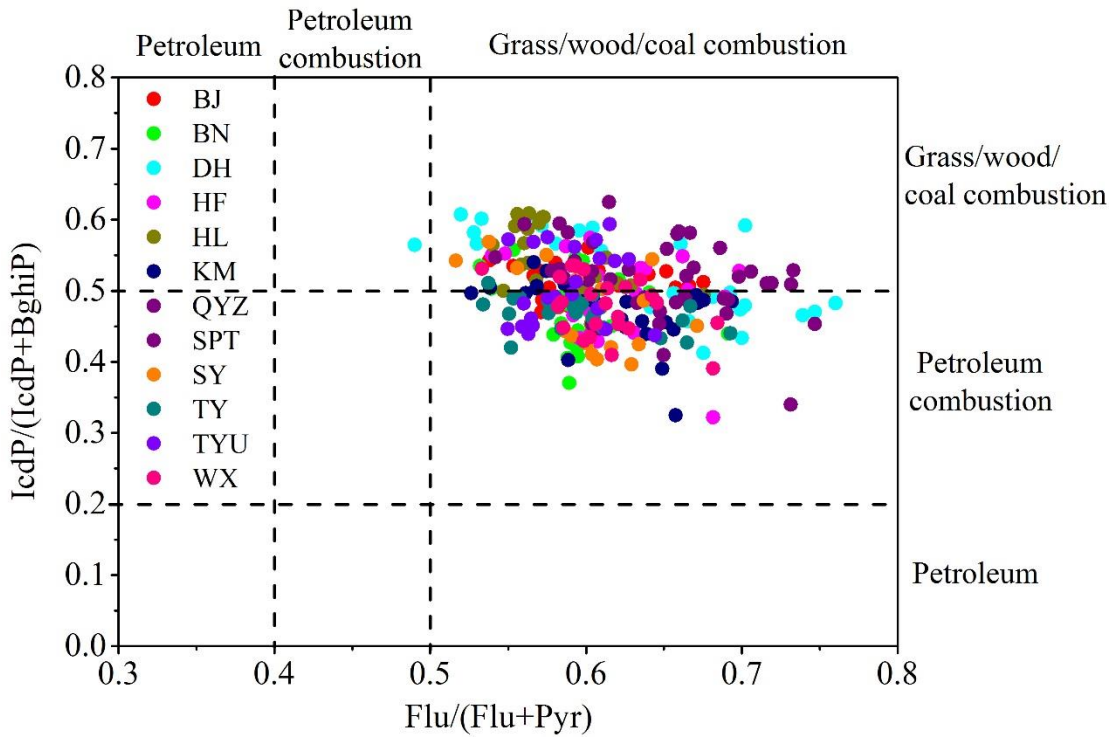

Figure 5 Diagnostic ratios of IcdP/(IcdP +BgiP) versus Flu/(Flu+Pyr) at 12 sites in China. Ranges of ratios for sources are adopted from Yunker et al. (2002).

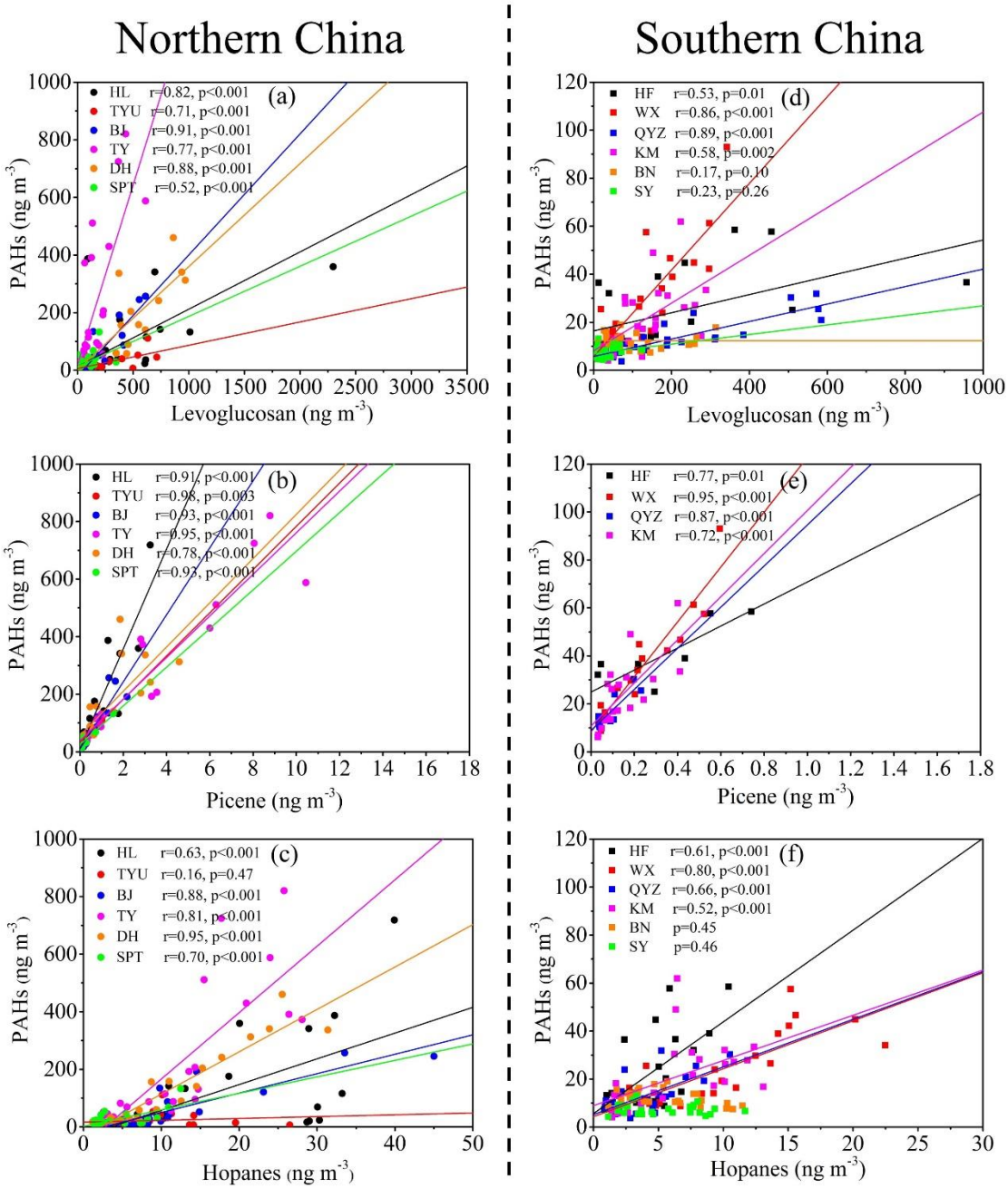

795

796 Figure 6 The correlation between PAHs and levoglucosan, picene and hopanes at sites in the

797 northern China (a-c) and the southern China (d-f).

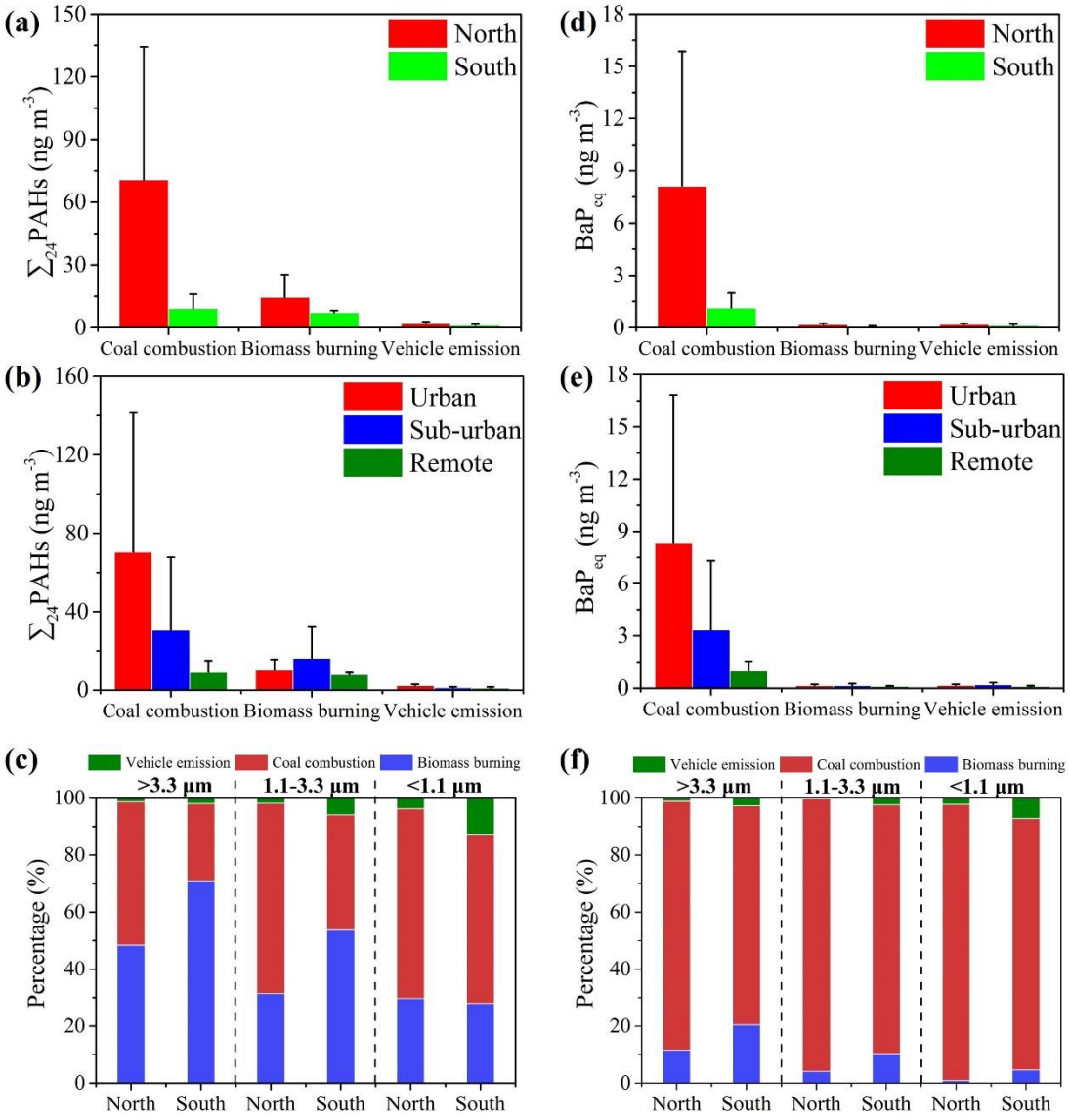

Figure 7 Source apportionment of $\sum_{24}$ PAHs and BaP$_{eq}$ in different regions (a, c), sampling sites (b, d) and size particles (c, f).

~~Figure 7 Source apportionment of atmospheric PAHs in the northern and the southern China.~~

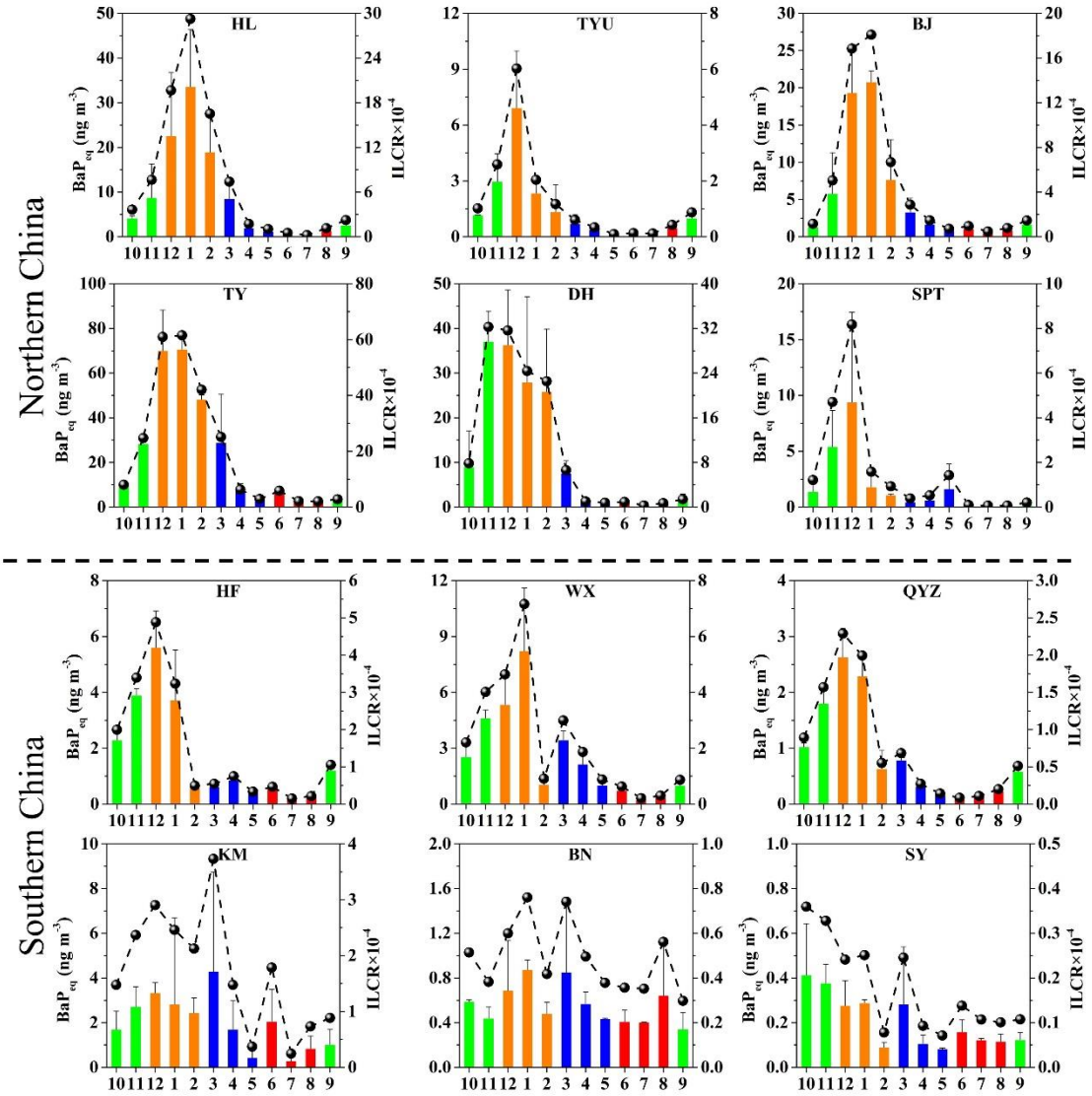

Figure 8 Monthly variations of BaP_{eq} and ILCR at sites in the northern China and the southern China. The green, yellow, blue and red bars represent BaP_{eq} in fall (October − November, 2012 and September, 2013), winter (December 2012 – February 2013), spring (March – May, 2013), and summer (June − AugustSeptember, 2013), respectively.

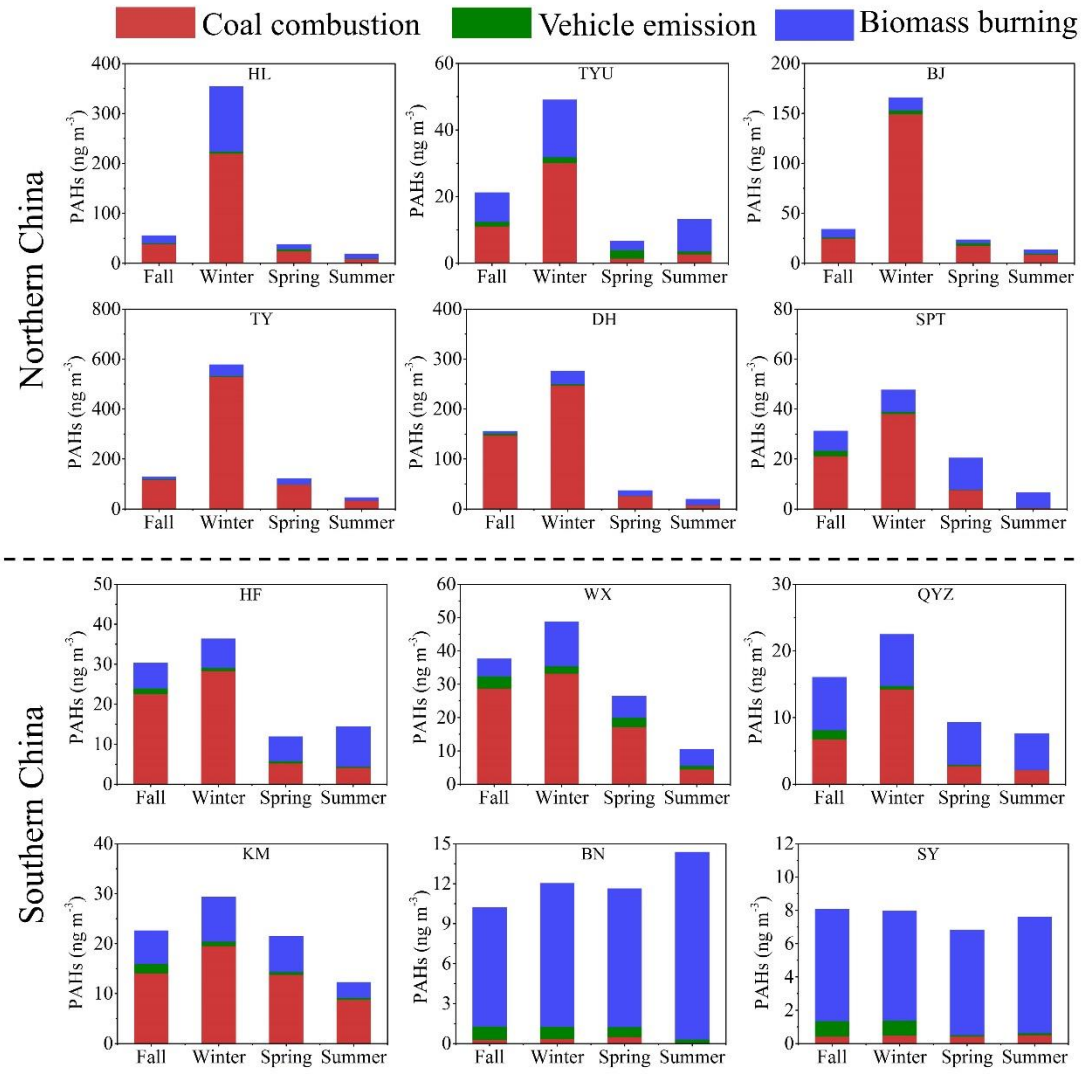

Figure 9 Seasonal variations of PAHs source contributions in China.